ELECTRODYNAMIC COUPLING OF THE MAGNETOSPHERE AND IONOSPHERE

ROBERT L. LYSAK

School of Physics and Astronomy, University of Minnesota, Minneapolis, MN 55455, U.S.A.

(Received 13 December, 1988)

Abstract. The auroral zone ionosphere is coupled to the outer magnetosphere by means of field-aligned currents. Parallel electric fields associated with these currents are now widely accepted to be responsible for the acceleration of auroral particles. This paper will review the theoretical concepts and models describing this coupling. The dynamics of auroral zone particles will be described, beginning with the adiabatic motions of particles in the converging geomagnetic field in the presence of parallel potential drops and then considering the modifications to these adiabatic trajectories due to wave-particle interactions. The formation of parallel electric fields can be viewed both from microscopic and macroscopic viewpoints. The presence of a current carrying plasma can give rise to plasma instabilities which in a weakly turbulent situation can affect the particle motions, giving rise to an effective resistivity in the plasma. Recent satellite observations, however, indicate that the parallel electric field is organized into discrete potential jumps, known as double layers. From a macroscopic viewpoint, the response of the particles to a parallel potential drop leads to an approximately linear relationship between the current density and the potential drop.

The currents flowing in the auroral circuit must close in the ionosphere. To a first approximation, the ionospheric conductivity can be considered to be constant, and in this case combining the ionospheric Ohm's Law with the linear current-voltage relation for parallel currents leads to an outer scale length, above which electric fields can map down to the ionosphere and below which parallel electric fields become important. The effects of particle precipitation make the picture more complex, leading to enhanced ionization in upward current regions and to the possibility of feedback interactions with the magnetosphere.

Determining adiabatic particle orbits in steady-state electric and magnetic fields can be used to determine the self-consistent particle and field distributions on auroral field lines. However, it is difficult to pursue this approach when the fields are varying with time. Magnetohydrodynamic (MHD) models deal with these time-dependent situations by treating the particles as a fluid. This class of model, however, cannot treat kinetic effects in detail. Such effects can in some cases be modeled by effective transport coefficients inserted into the MHD equations. Intrinsically time-dependent processes such as the development of magnetic micropulsations and the response of the magnetosphere to ionospheric fluctuations can be readily treated in this framework.

The response of the lower altitude auroral zone depends in part on how the system is driven. Currents are generated in the outer parts of the magnetosphere as a result of the plasma convection. The dynamics of this region is in turn affected by the coupling to the ionosphere. Since dissipation rates are very low in the outer magnetosphere, the convection may become turbulent, implying that nonlinear effects such as spectral transfer of energy to different scales become important. MHD turbulence theory, modified by the ionospheric coupling, can describe the dynamics of the boundary-layer region. Turbulent MHD fluids can give rise to the generation of field-aligned currents through the so-called α-effect, which is utilized in the theory of the generation of the Earth's magnetic field. It is suggested that similar processes acting in the boundary-layer plasma may be ultimately responsible for the generation of auroral currents.

Table of Contents

Space Science Reviews **52:** 33–87, 1990.

1. Introduction

It is well known that the aurora occurs on magnetic field lines along which field-aligned currents flow (e.g., Birkeland, 1908; Iijima and Potemra, 1976). The auroral Birkeland currents generally occur as two sheet currents, extended in longitude but narrowly confined in latitude, although the current systems at noon and midnight are more complex in structure. Nevertheless, the existence of the auroral current systems requires that currents flow across magnetic field lines in the ionosphere, and also at some location in the outer magnetosphere. In the collisional ionosphere, such cross-field currents require the existence of electric fields to drive them, implying that the ionosphere constitutes a load for the current system. Electromagnetic energy is, therefore, dissipated in the ionosphere, and so the maintenance of the current system requires the presence of the generator somewhere in the outer magnetosphere. Thus the auroral current system represents a means of tapping the kinetic or thermal energy of the magnetospheric plasma, and transporting it to the ionosphere where it is dissipated.

Part of this energy deposition in the ionosphere comes in the form of the primary electron beam with energy the order of 1–10 keV which excites atoms in the neutral atmosphere producing the auroral light (e.g., McIlwain, 1960). Although the source of these nearly monoenergetic electrons has been a controversial subject, it is now generally recognized that these electrons have passed through a parallel potential drop (Gurnett and Frank, 1973; Evans, 1974; Mozer *et al.*, 1980; but see also Bryant *et al.*, 1978; Whalen and Daly, 1979; Bingham *et al.*, 1984). The acceleration of these electrons constitutes another load on the field-aligned current system. The existence of this parallel potential drop itself must be explained, since in an ideal collisionless plasma the conductivity parallel to the magnetic field is infinite and so there should be no parallel electric field. However, although the auroral zone plasma is collisionless above the ionosphere, ideal conditions break down due to the finite number of electrons available to carry current, especially in the upward current region where downward moving electrons must overcome the magnetic mirror forces in the Earth's dipole field in order to precipitate into the ionosphere and contribute to the net field-aligned current.

Since the plasma density in the auroral zone can be quite low (e.g., Calvert, 1981), the drift velocity for a given level of current can be large. This can lead to the excitation

of plasma instabilities which can impede the adiabatic flow of particles. Nonlinear effects due to these excited plasma waves can give rise to parallel electric fields. Such effects are often parameterized by an effective resistivity in the plasma (Mozer, 1975; Papadopoulos, 1977). This description is a bit misleading, however, since satellite observations show that the parallel electric field does not occur as a smooth monotonic field, but rather as a series of localized potential steps, known as double layers (Temerin *et al.*, 1982; Koskinen *et al.*, 1988; Boström *et al.*, 1988). These double layers arise from plasma turbulence due to the trapping of electrons and ions in localized potential bumps or dips. Plasma turbulence effects also manifest themselves in the production of transversely heated ions, which form conic-shaped distributions in velocity space as they propagate in the mirror field of the Earth (see Chang *et al.*, 1986).

Whatever the source of the parallel electric field, the motion of charged particles under the combined effect of the electric field and the mirror field can give rise to a relationship between the potential drop, the mirror ratio between the source of the particles and the ionosphere, and the current density of the precipitating electrons. Under conditions that are easily satisfied in the auroral zone, this relationship is approximately linear (Lyons *et al.*, 1979; Fridman and Lemaire, 1980). This linear relationship has been shown to exist in cases when the current is mainly carried by runaway particles whose orbits are adiabatic.

The requirement that the auroral current system close in the ionosphere can influence the structure of the current systems themselves. The ionospheric currents consist of Pedersen currents parallel to the electric field in the ionosphere, and Hall currents which are perpendicular to both the electric and magnetic field. In the case when the ionospheric conductivity is uniform, only the Pedersen currents can close the field-aligned current system. When combined with the linear current density-voltage relation mentioned above, the Pedersen conductivity gives rise to a critical scale size for the aurora, which is the order of 100 km for typical auroral parameters (Chiu and Cornwall, 1980). This scale represents the maximum scale on which parallel electric fields are significant. On larger scales, the electric fields in the magnetosphere simply map to the ionosphere, and magnetic field lines are equipotentials. When the ionospheric conductivity is allowed to vary in time, a feedback instability can be set up which can give rise to increasing structure in the current system (Sato, 1978).

These elements of auroral current systems have been synthesized into a variety of models for auroral flux tubes, which generally fall into two classes. Kinetic models emphasize the adiabatic motions of particles originating in both the magnetosphere and ionosphere (Chiu and Schulz, 1978; Lyons, 1980; Chiu and Cornwall, 1980). The parallel potential drop is determined from the individual particle populations by means of quasi-neutrality, or in some cases, Poisson's equation. By varying the relative densities of various particle populations, different electric field structures can be found. While these models have had success in describing the steady-state structure of the large-scale inverted-V regions, they are not easy to generalize to the time-dependent case. In this case, it is useful to consider the fluid nature of the plasma by using the magnetohydrodynamic (MHD) approach. The main disadvantage here is that, as noted

above, the MHD equations for a collisionless medium do not allow parallel electric fields. This deficiency can be remedied, or at least patched up, by assuming an effective resistivity in regions of strong field-aligned current. Although somewhat *ad hoc*, this procedure allows the study of the effects of parallel electric field on the propagation of Alfvén waves between the magnetosphere and ionosphere. These Alfvén waves are manifested in the observation of micropulsations in the auroral zone. Such models also allow the study of the magnetospheric response to changes in the ionosphere such as those produced by the ionospheric feedback instabilities mentioned above.

The structure of the auroral current system is strongly influenced by the flow of plasma in the outer magnetosphere, which can generate the field-aligned currents. Such generators can be grouped loosely into current generators, which deliver a fixed current independent of the ionospheric response, and voltage generators, which deliver a fixed potential drop (Lysak, 1985). The real generator is clearly somewhere in between these two extremes, and must be analyzed by considering the dynamics of plasma flow in the boundary-layer and plasma sheet regions which connect to auroral field lines. This situation is complicated by the fact that these generator regions are often turbulent, and energy transfer between structure at various scales must be taken into account, as must the reaction of the ionosphere on the boundary-layer dynamics.

The remainder of this review is organized as follows: in Section 2, the motions of single particles in the auroral electric and magnetic fields is analyzed, for both adiabatic situations and in the case where wave-particle interactions may modify the particle orbits. Section 3 will discuss the formation of parallel electric fields on auroral field lines, and Section 4 will consider the effects of the ionosphere. In Section 5, coupling in time-dependent situations will be reviewed and the propagation of Alfvén waves in the auroral zone will be discussed. Section 6 will discuss the generator of the auroral current system. Results will be summarized in Section 7.

2. Particle Motions

In this section, we will briefly discuss the motion of charged particles on auroral field lines. These particles are affected primarily by the magnetic mirror field of the Earth, as well as any parallel potential drop which may occur on the auroral field line. In addition, wave turbulence can affect the particle motions, and change the adiabatic invariants of the particles. This chapter is not meant to be a comprehensive review of auroral particle motions, but rather to set the framework for subsequent discussion. For a detailed review of plasmas in the auroral zone, the reader is referred to Chiu *et al.* (1983).

2.1. Adiabatic motions

To start, let us consider that we have as given a certain value of the parallel potential drop, and ask what the response of auroral zone electrons and ions should be. If we assume that the particles move adiabatically, their motion can be characterized by two

constants of the motion, their energy:

$$E = \tfrac{1}{2}mv^2 + q\Phi \tag{1}$$

and magnetic moment:

$$\mu = \frac{mv_\perp^2}{2B} \,. \tag{2}$$

If we combine these two relations, we can describe the parallel motion of a charged particle by means of an effective one-dimensional potential

$$E = \tfrac{1}{2}mv_\parallel^2 + U \,, \tag{3}$$

where

$$U = \mu B + q\Phi \,.$$

Given these invariants, we can see that if a particle moves from a place where the magnetic field is B_0 and the parallel potential is Φ_0 to a place with magnetic field B and potential Φ, its perpendicular and parallel velocities will be given by

$$v_\perp = v_{\perp,0}\sqrt{\frac{B}{B_0}} \,, \qquad v_\parallel = \pm\sqrt{v_{\parallel,0} - (2/m)\left[\mu(B - B_0) + q(\Phi - \Phi_0)\right]} \,. \tag{4}$$

It can be seen that not all regions along the field line will be accessible to the particle since at some points the parallel velocity as given above may become imaginary. These inaccessible regions can be easily seen if we plot the effective potential U for electrons and ions, as is done in Figure 1 for the case when the ionospheric potential is higher than that in the outer magnetosphere.

These accessibility conditions divide the particle distributions into distinct regions, as are illustrated in Figure 2. In this figure, and in the subsequent discussion, we will assume that the parallel electric field is directed upwards, as is the case in the primary auroral acceleration region. The same results can be applied to a region of downward electric field, with the roles of electrons and ions being reversed.

Plasma sheet electrons with large perpendicular energy will be reflected before reaching the ionosphere by the magnetic mirror force. Plasma sheet electrons which are more field-aligned will, however, reach the ionosphere where they will be lost due to collisions, forming a precipitating population. Ionospheric electrons will appear in the upgoing region if they are energetic enough, but will be reflected by the electrostatic potential if they are too low in energy. In addition, there is a region of the electron velocity space in which the electrons are trapped between the magnetic mirror below and the electrostatic mirror above. This region can only be populated by electrons which have been scattered into the region by wave-particle interactions. For ions in an upward electric field the situation is simpler since the electrostatic and magnetic mirror forces are in the same direction and so the effective potential (Figure 1) is monotonic. Here we have also

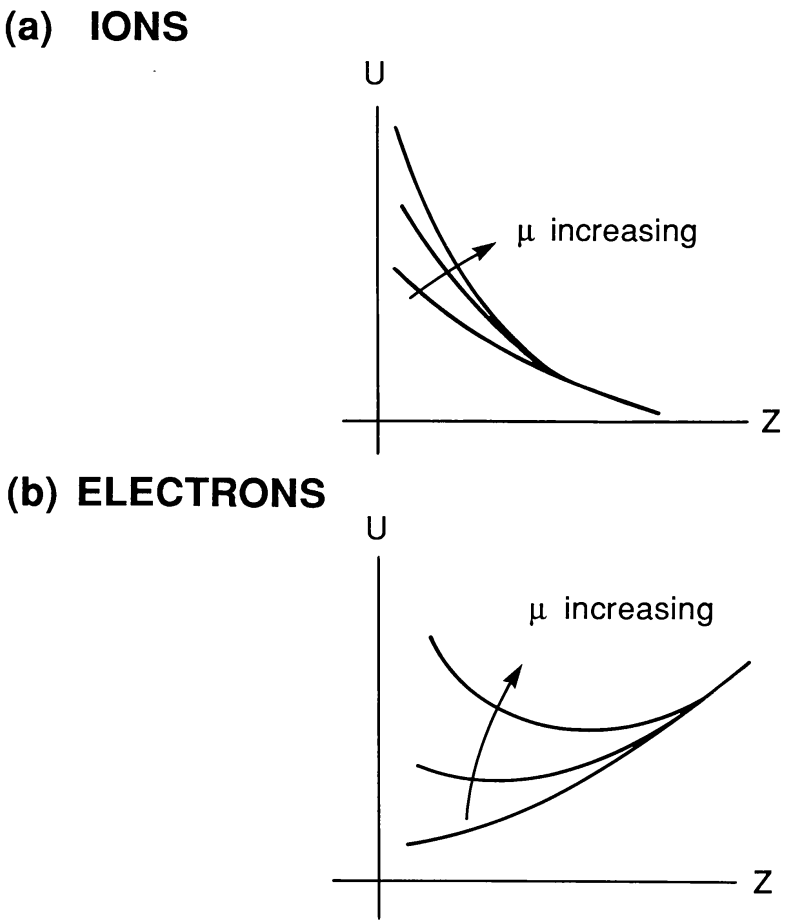

Fig. 1. Effective potentials for ions (a) and electrons (b) on an auroral field line in which the electrostatic potential is higher at the ionosphere than in the outer magnetosphere. As the magnetic moment μ increases, the ions are more strongly repelled by the ionosphere while the trapping of electrons in a potential minimum becomes possible.

reflected and precipitating plasma sheet ions, but ionospheric ions can only populate the upgoing loss cone.

These phase space boundaries have been successfully used to determine the magnitude of the parallel potential drop both below and above the satellite position (Mizera and Fennell, 1977; Whipple, 1977; Croley *et al.*, 1978; Chiu and Schulz, 1977). The existence of a potential drop below the satellite can be most clearly determined by the presence of an ion beam, which populates the upgoing loss cone region in Figure 2. The energy at the peak of the ion beam distribution corresponds to the potential drop that the ion beam has fallen through if the ion orbits are adiabatic. Information about the parallel potential below the satellite can also be determined from examination of the upgoing electron loss cone. In the absence of the potential drop, the edge of the loss cone is at a fixed pitch angle given by $\sin\alpha = \sqrt{B/B_I}$, where α is the loss cone angle, and B and B_I are the magnetic field strengths at the satellite and the ionosphere, respectively. In the presence of a parallel potential, the loss cone boundary, as determined by the location at which electrons mirror just above the ionosphere, is given by $\sin\alpha = \sqrt{(B/B_I)\,(1 + e\Delta\Phi/W)}$, where W is the kinetic energy of the electron. Thus the

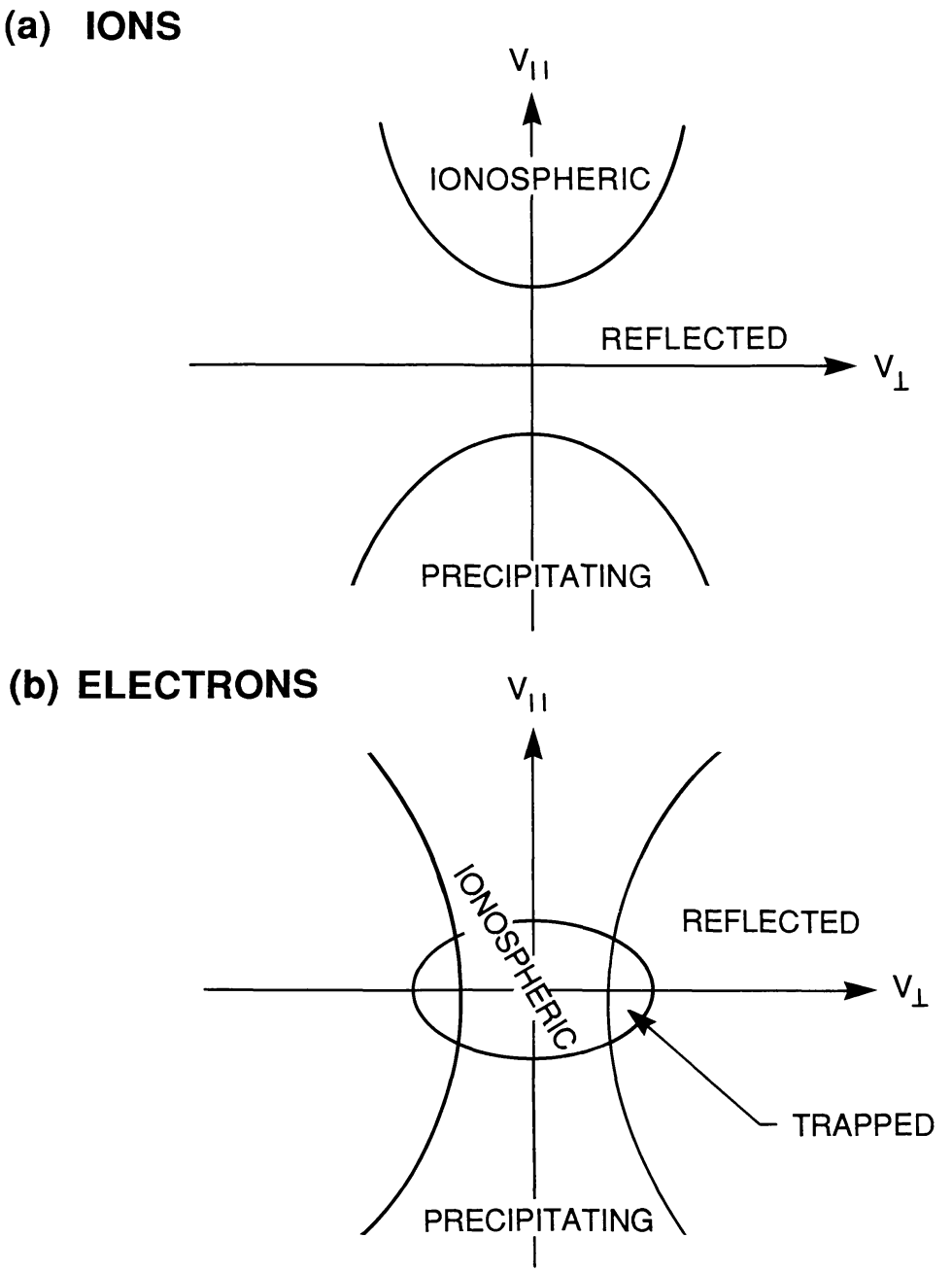

Fig. 2. Velocity space plots for ions (a) and electrons (b) for the same situation as Figure 1. Accessibility conditions lead to different regions of velocity space being populated by reflected magnetospheric ions, precipitating ions, and upgoing ionospheric ions. Similar populations of electrons can be found but now ionospheric electrons can be reflected back toward the ionosphere, and a region of electrons trapped between the electrostatic mirror above and the magnetic mirror below can be found.

electron loss cone widens at lower energy in the presence of a parallel potential drop. The ions and electron distributions can thus give independent estimates of the potential drop below the satellite.

The electron population can be used to determine the potential above the satellite. If a downgoing electron beam is present, the energy of these electrons is indicative of the parallel potential drop. In addition, for energies less than the potential drop above the satellite, a backscattered population of ionospheric electrons is present which is

symmetric between upgoing and downgoing electrons and occupies the region within the ellipse in Figure 2(b) (Evans, 1974). In some cases, a population of electrons trapped between the magnetic mirror below and the electrostatic mirror above the satellite can be observed (e.g., Mizera and Fennell, 1977). This population gives information about the potential above and below the satellite since, for $v_\parallel = 0$, this population extends from perpendicular energies of $e\Delta\Phi_B/[(B_I/B) - 1]$ to $e\Delta\Phi_A/[1 - (B_0/B)]$ where $\Delta\Phi_B$ and $\Delta\Phi_A$ are the potential drops below and above the satellite, respectively, and B_0 is the field strength at the source.

The total current produced by the adiabatic motion of particles was discussed by Knight (1973), Lemaire and Scherer (1973, 1974), and Fridman and Lemaire (1980), who treated a distribution of particles which was an anisotropic Maxwellian at the source, presumably created by strong pitch-angle scattering, which developed a loss cone as it propagated to lower altitudes. Considering only the electrons as charge carriers, this procedure yields a parallel current density given by

$$j_\parallel = -n_e e \left(\frac{T_\parallel}{2\pi m_e}\right)^{1/2} \frac{B_I}{B_0}\left[1 - \frac{\exp(-xe\Delta\Phi/T_\parallel)}{1 + x}\right], \tag{5}$$

where $x = (T_\parallel/T_\perp)/(B_I/B_0 - 1)$, n_e, $T_\parallel$, and $T_\perp$ are the density, and parallel and perpendicular temperatures of the electrons at the source, and $\Delta\Phi$ is the field-aligned potential drop. Here positive current corresponds to downward currents, and positive $\Delta\Phi$ occurs when the source potential is greater than the ionospheric potential. While this functional form is somewhat complicated, it is worth noting that for $1 \ll e\Delta\Phi/T_\parallel \ll x^{-1}$, this relationship simplifies to a linear relationship

$$j_\parallel = -K\Delta\Phi, \tag{6}$$

where the effective conductance density K is given by

$$K = \frac{n_e e^2}{T_\perp(1 - B_0/B_I)}\left(\frac{T_\parallel}{2\pi m_e}\right)^{1/2}. \tag{7}$$

For reasonable parameters, e.g., $T_\parallel = T_\perp = 100$ eV and $B_I/B_0 = 1000$, this linear relationship holds for potential drops between 100 eV and 100 keV, encompassing nearly the entire region of interest for the auroral zone.

This approximately linear current-voltage relationship has been put to an observational test by Lyons *et al.* (1979) who compared the potential drop as determined from the peak of the auroral electron energy distribution with the energy flux of the precipitating electrons. When the potential drop is much greater than the thermal energy of the source plasma, the energy flux ε is given by $\varepsilon = -e\Delta\Phi j_\parallel$, and so, if the linear current-voltage relation (6) holds, the energy flux is $\varepsilon = eK\Delta\Phi^2$. Comparison of the precipitating electron flux and potential drop with obsevations from rocket flights showed that this relation held reasonably well, although there was some dependence on the minimum energy used to determine the energy flux.

2.2. Wave-particle interactions

The adiabatic motions described in the preceding sub-section are valid only as long as the electric and magnetic fields are slowly varying in space and time. Waves excited by various sorts of plasma instabilities can interact with auroral zone particles in such a way as to violate these invariants. A variety of wave modes, from hydromagnetic waves with periods of many minutes to auroral radio emissions at frequencies of several hundred kilohertz, have been observed in the auroral zone. The vast zoo of plasma waves will not be reviewed here. A survey of the types of plasma waves observed in the magnetosphere has been given by Shawhan (1979). A review of hydromagnetic waves in the magnetosphere was given by Southwood and Hughest (1983). A collection of articles on the acceleration of ions in the magnetosphere can be found in the book edited by Chang *et al.* (1986).

Transverse ion acceleration processes have been reviewed previously (Lysak, 1986) and so will not be discussed in detail here. Evidence for wave-particle interactions is found from the acceleration of both ion conics and beams, since the ion beams observed have transverse energies much greater than the typical ionospheric temperatures (e.g., Ghielmetti *et al.*, 1986). In addition, it has been noted that downgoing ion beams are not observed throughout most of the auroral zone (Ghielmetti *et al.*, 1979), indicating that wave-particle interactions modifying the adiabatic ion orbits are operating along the auroral flux tube. Evidence for a parallel interaction between hydrogen and oxygen ions has been found by S3–3 (Ghielmetti *et al.*, 1986) and Dynamics Explorer (Reiff *et al.*, 1986) indicating that the hydrogen ions had somewhat less energy than the parallel potential drop inferred from the electron distribution (see above), while oxygen ions had more energy. This has been interpreted as being the result of a H^+–O^+ streaming instability which draws on the free energy of the hydrogen beam and is damped on the ions (Bergmann and Lotko, 1986; Kaufmann *et al.*, 1986, Bergmann *et al.*, 1988).

Turning to electron effects, observed particle distributions show that purely adiabatic orbits cannot account for all features of observed distributions. For example, the trapped particle region indicated in Figure 2(b) is inaccessible to either the magnetospheric or ionospheric sources, and so should be empty. The observations of particles in this region (e.g., Mizera and Fennell, 1977) indicate that some wave scattering can take place. It is usually the case that the loss cone boundaries are not sharply defined, but are rather smooth, since pitch-angle scattering can scatter particles across these boundaries. Such pitch-angle scattering may be associated with the generation of auroral kilometric radiation which, accoridng to the widely accepted theory of Wu and Lee (1979), is driven by the free energy in these loss cones.

Some features of auroral precipitation are not easily explained by adiabatic processes. Fluctuations in the auroral precipitation have been noted since early observations by Evans (1967) and Arnoldy (1970). More recently, Johnstone and Winningham (1982) detected time-varying electron fluxes which were termed suprathermal electron bursts. Such bursts may have very low perpendicular temperatures, with a relatively flat distribution in parallel velocity, indicating that some form of parallel heating has taken

place (McFadden *et al.*, 1986, 1987). Indeed, the existence of these classes of auroral precipitation has led some authors to question whether field-aligned potential drops are necessary at all and to formulate models to energize the auroral electrons totally from wave acceleration (Bryant *et al.*, 1978; Whalen and Daly, 1979; Bingham *et al.*, 1984).

From a theoretical viewpoint, the dominant wave-particle effect of importance to magnetosphere-ionosphere coupling is the effective resistivity associated with the excitation of waves from the electron free energy. If instabilities associated with the electron current are responsible for the transverse ion acceleration, the energy for this acceleration must come from the driving electrons. In the weakly turbulent case, the quasi-linear theory gives one framework to discuss this anomalous resistivity (see review by Papadopoulos, 1977). Although this theory applied to observed levels of electrostatic ion-cyclotron (EIC) waves can give reasonable estimate of the parallel electric field required to explain the auroral potential drop (Hudson *et al.*, 1978), it does not appear sufficient since electron runaway limits the effectiveness of this mode. In addition, the EIC waves are observed to be coherent, invalidating the assumptions of quasi-linear theory. In this case, electron trapping becomes a way in which the EIC waves can impede the flow of electrons (Lysak and Hudson, 1979).

Electron trapping is not completely efficient at preventing runaway, and it has been suggested that further resistivity can be provided by the scattering of electrons at the anomalous cyclotron resonance (Rowland *et al.*, 1981; Rowland and Palmadesso, 1983). In this scenario, the electrons which escape trapping by EIC waves are accelerated until they reach a critical velocity $v_{\|} = (\omega + \Omega_e)/k_{\|}$ at which they can resonate with whistler mode waves. At this point, the electrons can be pitch-angle scattered, isotropizing the electrons and reducing their parallel velocity. This model appears to be in qualitative agreement with AE–D observations (Lin and Rowland, 1985) which show that field-aligned electron fluxes tend to become isotropic beginning at low energies in agreement with simulations based on the anomalous cyclotron mechanism.

Recent satellite observations from S3–3 (Temerin *et al.*, 1982) and Viking (Boström *et al.*, 1988; Koskinen *et al.*, 1988) have indicated that the parallel electric field is localized into discrete pulses known as double layers. These structures, which will be discussed more completely in the next section, consist of two pulses of oppositely directed parallel electric field, with the upward pulse being stronger than the downward pulse (in upward field-aligned current regions). The reversed electric field structure allows the trapping of electrons, and thus leads to another form of wave-particle acceleration of electrons, termed diffusive acceleration by Lotko (1986). The trapping and subsequent runaway of low-energy electrons can give rise to field-aligned particle distributions on the edge of auroral arcs, as was discussed above (McFadden *et al.*, 1986).

It is worth pointing out that the validity of the adiabatic current-voltage relationship (6) does not rule out the existence of wave-particle interactions nor the development of double-layer electric fields. In fact, this relationship says nothing about the formation of the parallel potential drop, only its effect on the precipitating particles. Double layers

or wave turbulence mainly affect low-energy electrons while the higher energy particles which can carry the bulk of the precipitation flux remain adiabatic (cf. Lotko, 1986). An observer in the ionosphere will mostly see particles which pass through the acceleration region adiabatically. Thus, the existence of this current-voltage relationship does not necessarily imply that wave-particle interactions are not important in the production of parallel potential drops. In fact, it has been shown (Lysak and Hudson, 1987) that a global linear current-voltage relationship can arise from a local model of anomalous resistivity.

3. Parallel Electric Fields

It has long been known that the discrete aurora is associated with nearly monoenergetic beams of electrons with energy the order of 10 keV which impact the ionosphere (e.g., McIlwain, 1960). Despite this well-known result, it was not until over a decade later that it became firmly established that this energization was associated with an electric field parallel to the magnetic field (Mozer and Fahleson, 1970; Gurnett and Frank, 1973; Evans, 1974; Mozer *et al.*, 1977, 1980). This lack of belief in parallel electric fields stemmed from the fact that the auroral zone plasma was collisionless and so the resistivity along the field lines was infinite. This line of reasoning, derived from a MHD picture of the auroral plasma, was misleading primarily because of the low density of charge carriers. As a result, the maximum current that could be carried by electrons would be of the order of nev_e, where n is the density. For plasma sheet or boundary-layer parameters of $n = 1\ \mathrm{cm}^{-3}$ and $T = 100$ eV, this limiting current is of the order of $1\ \mu\mathrm{A\ m}^{-2}$, comparable to typical auroral currents. This current limitation is especially important for upward currents carried by precipitating electrons since the electrons must overcome the mirror force to precipitate, further reducing the current which can flow. As noted in the previous chapter, the presence of a parallel electric field can increase the number of electrons which can precipitate. This has led to a class of models which attempt to model the parallel electric field by determining the electric field necessary to maintain quasi-neutrality.

In addition, when the drift velocity between ions and electrons approaches the electron thermal speed, a variety of plasma instabilities can be set up which may lead to an anomalous resistivity, as discussed above. Kindel and Kennel (1971) have pointed out that the electrostatic ion-cyclotron (EIC) instability is the most easily destabilized by the auroral current, at least under the condition that the ion and electron temperatures are equal. This mode has, therefore, often been assumed to contribute to the resistivity. As noted above, however, EIC turbulence is not very effective at completely trapping the electron population. Satellite observations show that, in contrast to a weak turbulence theory which would produce a smooth electric field, the parallel electric field consists of a series of small, localized parallel electric field pulses known as double layers.

Thus theories of parallel electric field consists on one hand of the attempts to model the macroscopic current system self-consistently, and on the other of studies of how parallel electric fields arise from microscopic effects. We will proceed to investigate both of these approaches.

3.1. Macroscopic models

As noted above, the presence of the mirror geometry of the geomagnetic field, in combination with the low density of potential current carrying electrons, leads to a restriction on the amount of current which can flow out of the ionosphere. The early model of Alfvén and Fälthammar (1963) considered monoenergetic populations of ions and electrons with different pitch angles, and used quasi-neutrality to determine the parallel potential drop. If a population of electrons exists in the source, where the magnetic field is B_0, with parallel and perpendicular energies $W_{e\parallel}$ and $W_{e\perp}$, and a similar population of ions exists, then quasi-neutrality is maintained for a parallel electric field

$$E_{\parallel} = -K \frac{\mathrm{d}B}{\mathrm{d}s} , \tag{8}$$

where s is the distance along the field line and K is given by

$$K = \frac{W_{i\parallel} W_{e\perp} - W_{e\parallel} W_{i\perp}}{eB_0(W_{i\parallel} + W_{e\parallel})} , \tag{9}$$

where all quantities refer to the source population. This model produces potential drops far greater than what is observed in the auroral zone, primarily because of the neglect of ionospheric particles which could neutralize the plasma sheet populations. In spite of this shortcoming, it does indicate two features common to potential drops supported by the magnetic mirror: the parallel electric field is proportional to the magnetic field gradient, and the potential drop vanishes if the electrons and ions have the same pitch angle. Using a general distribution function at the source, Persson (1963, 1966) showed that the parallel electric field vanishes if the electrons and ions have the same pitch-angle distribution.

A more detailed analysis of the effects of adiabatic particle motion in the mirror field was undertaken by the Aerospace group (Chiu and Schulz, 1978; Chiu and Cornwall, 1980; Chiu *et al.*, 1981; Newman *et al.*, 1986). In this model, source populations of magnetospheric and ionospheric ions and electrons were assumed, and the potential drop was determined self-consistently, first from quasi-neutrality (Chiu and Schulz, 1978) and in the later works from Poisson's equation. This procedure allowed not only the determination of the total potential drop, but also the distribution of the parallel electric field as a function of altitude could be determined. It was found that the potential scaled roughly as the magnetic field strength, i.e., the parallel electric field was proportional to the magnetic field gradient, as in the earlier work of Alfvén and Fälthammar (1963). However, due to the presence of the ionospheric populations, the total potential drop is not as high as in that previous work. In the models presented by Chiu and Schulz (1978), the maximum parallel electric field was of the order of $0.4\ \mathrm{mV\ m^{-1}}$ and occurred at altitudes less than 2500 km.

While all of these models considered only the adiabatic motions of particles, the effect of turbulence was included in a phenomenological way by Cornwall and Chiu (1982). They noted that auroral zone turbulence can heat ions transversely to the magnetic field,

as noted in the previous chapter. This ion heating tends to reduce the differential pitch-angle anisotropy between the ions and electrons. As can be seen from Equation (9), this heating tends to reduce the parallel potential drop. Thus turbulence tends to shut off the mirror supported electric field. However, Cornwall and Chiu (1982) also argue that anomalous resistivity models are too dissipative to support the potential drop. This assertion will be discussed later in this review, when we consider the energy sources for the auroral current system.

3.2. Microscopic processes

When the relative drift velocity between electrons and ions reaches a fraction of the electron thermal speed, low-frequency instabilities can be excited. Kindel and Kennel (1971) showed that for a hydrogen plasma with $T_e = T_i$, EIC waves should be excited for drifts $V_D \geq 13a_i = 0.3a_e$, where $a_s = \sqrt{2T_s/m_s}$ is the thermal speed for species s. For heavier ions, the critical drift decreases, scaling roughly as $m^{-1/2}$. For equal temperatures, the ion-acoustic instability is damped strongly by the ions, and the critical drift is the order of the electron thermal speed. When $T_e \gg T_i$, however, the EIC threshold decreases only weakly but the ion-acoustic mode becomes more unstable, with V_D/c_s approaching 1 for $T_e/T_i \geq 10$. Thus in the hot electron regime the ion-acoustic instability will dominate. While at first glance, one might assume that the ion and electron temperatures are roughly equal in the topside ionosphere, this situation might change above a pre-existing region of upward parallel electric field since the cold ionospheric electrons will not be able to overcome the potential drop while ionospheric ions can. Since good measurements of the thermal plasma in the topside auroral ionosphere are rare, this question remains open.

EIC waves are in fact observed at large amplitudes in the auroral zone (Kintner *et al.*, 1978, 1979; Mozer *et al.*, 1980; Peterson *et al.*, 1986; André *et al.*, 1987) with typical amplitudes being $e\Phi/T_e \approx 0.4$. This level is consistent with wave saturation by resonance broadening (Dum and Dupree, 1970) and leads to an effective resistivity of $\nu^* = 0.4\Omega_i$, where ν^* is the effective collision frequency and Ω_i is the ion gyrofrequency (Lysak and Dum, 1983). This level of resistivity is sufficient to explain the auroral potential drop: taking $n = 10\ \mathrm{cm}^{-3}$ and $B = 0.5$ G yields a resistivity of 680 ohm-m, or a parallel electric field of $1.4\ \mathrm{mV\ m}^{-1}$ for a current of $2\ \mu\mathrm{A\ m}^{-2}$. Thus a region of parallel electric field of a few thousand kilometers will yield a potential drop of a few kilovolts.

As noted above, the usual quasi-linear estimates of resistivity associated with wave turbulence are inadequate to explain to observations of localized parallel electric fields observed by satellites (Temerin *et al.*, 1982; Koskinen *et al.*, 1988; Boström *et al.*, 1988). These double-layer fields are characterized by a localized spike of electric field, often accompanied by a smaller spike of electric field in the opposite direction (Figure 3). The net potential drop over one such structure has $e\Phi/T_e \approx 1$. Regions of what might be called double-layer turbulence contain a string of these pulses accompanied by pairs of equal amplitude oppositely directed spikes which contain no net potential which are referred to as solitary waves. The observed solitary waves and double layers as seen by

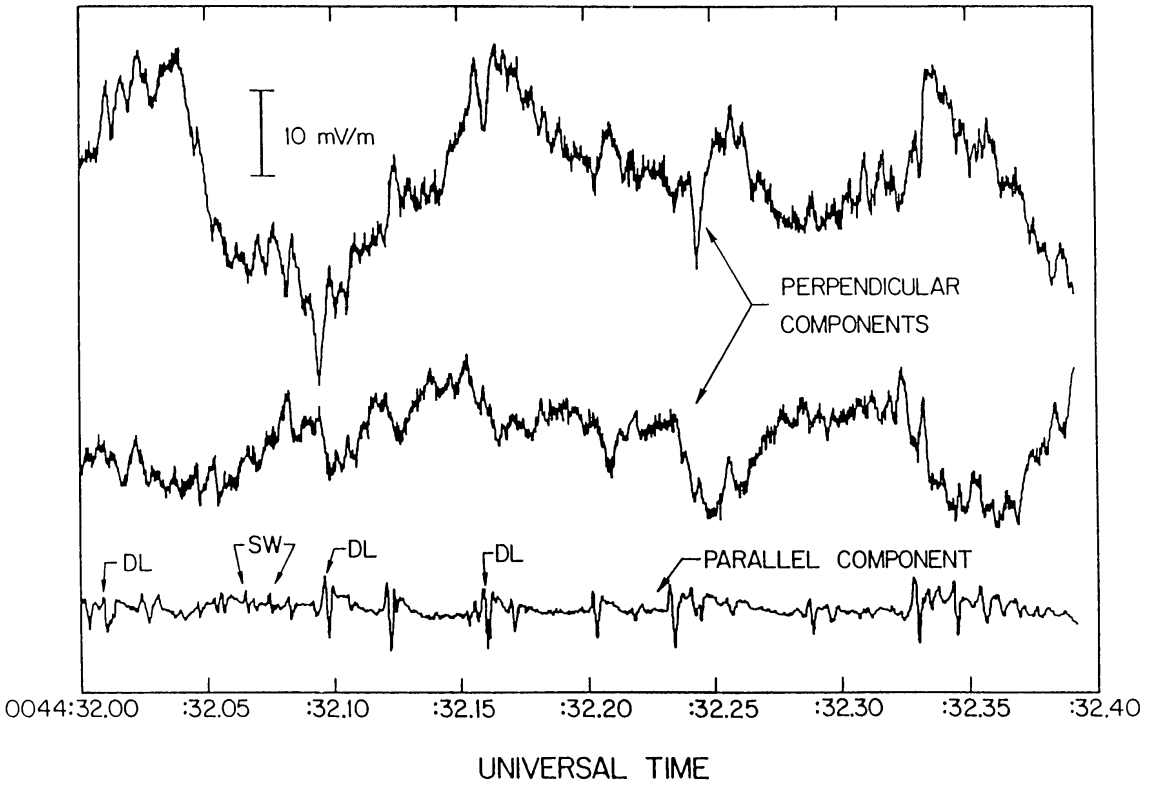

Fig. 3. Electric field data from the S3-3 satellite decomposed into the two perpendicular (*top*) and parallel (*bottom*) components. Examples of double layers (DL) and solitary waves (SW) are indicated. These data were taken on 11 August, 1976 at an altitude of 6030 km, an invariant latitude of 74.1° and a local time of 15.74 hours (from Temerin *et al.*, 1982).

electric field measurements could be interpreted either as upgoing density holes or downward propagating density enhancements (Temerin *et al.*, 1982). Fortunately, the Viking measurement allowed for simultaneous measurement of the three-dimensional electric field and density, and confirmed that these structures were upward going with speeds of 5–50 km s^{-1} and rarefactive, with $|\delta n/n| \approx 50\%$ (Koskinen *et al.*, 1988; Boström *et al.*, 1988), implying a potential structure as shown in Figure 4.

The theory of double layers is usually addressed within the framework of the so-called BGK theory (Bernstein *et al.*, 1957). This theory is based on the fact that a one-dimensional, electrostatic plasma must satisfy Poisson's equation:

$$\frac{\partial^2 \Phi}{\partial x^2} = -4\pi \sum_s q_s n_s , \tag{10}$$

where q_s and n_s are the charge and density of each species. Poisson's equation has the same form in one dimension as the usual particle equation of motion $\ddot{x} = -\partial U/\partial x$ where U is the potential energy per unit mass of the particle. As is well known, the first integral of the particle equation of motion gives the conservation of energy for the particle, and so a sketch of the potential energy U as a function of x gives the allowed regions of motion and the turning points for the particle.

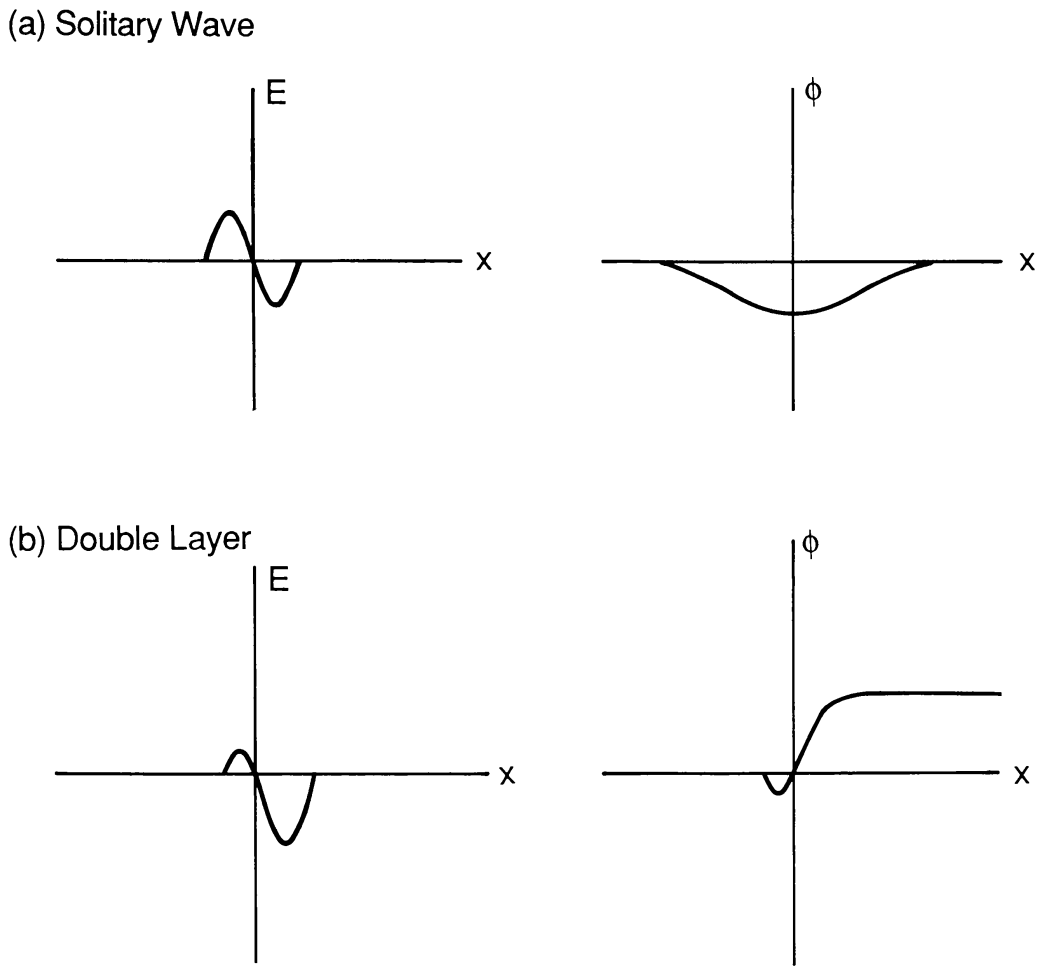

Fig. 4. Schematic drawing of electric field and potential patterns for (a) solitary waves, and (b) double layers.

In the case of Poisson's equation, a similar procedure can be carried out if the density of each species can be determined as a function of the electrostatic potential Φ. Then comparison of Poisson's equation with the equation of motion indicates that the effective potential (often termed the Sagdeev potential) can be written:

$$U(\Phi) = U(0) + \int_0^{\Phi} d\Phi' \, 4\pi \sum_s q_s n_s(\Phi') \,. \tag{11}$$

Then the energy equation takes the form

$$\frac{1}{2}\left(\frac{\partial \Phi}{\partial x}\right)^2 + U(\Phi) = U(0) \,. \tag{12}$$

A formal solution for the potential then gives

$$x - x_0 = \pm \frac{1}{\sqrt{2}} \int_0^{\Phi} \frac{d\Phi'}{\sqrt{|U(\Phi') - U(0)|}} \,. \tag{13}$$

While the direct procedure as outlined above can be carried out, in practice a form for the electrostatic potential is assumed, which implies a form for the Sagdeev potential. Then appropriate distribution functions can be found which self-consistently produce this potential. The 'classic' double-layer solution (Block, 1972) consists of a cold electron beam and a hot ion population incident on the low-potential side and a cold ion beam and a hot reflected electron population incident from the high-potential side (see Figure 5). These particle populations can self-consistently produce a step in the potential, with, however, some restrictions on the plasma parameters. For example, in

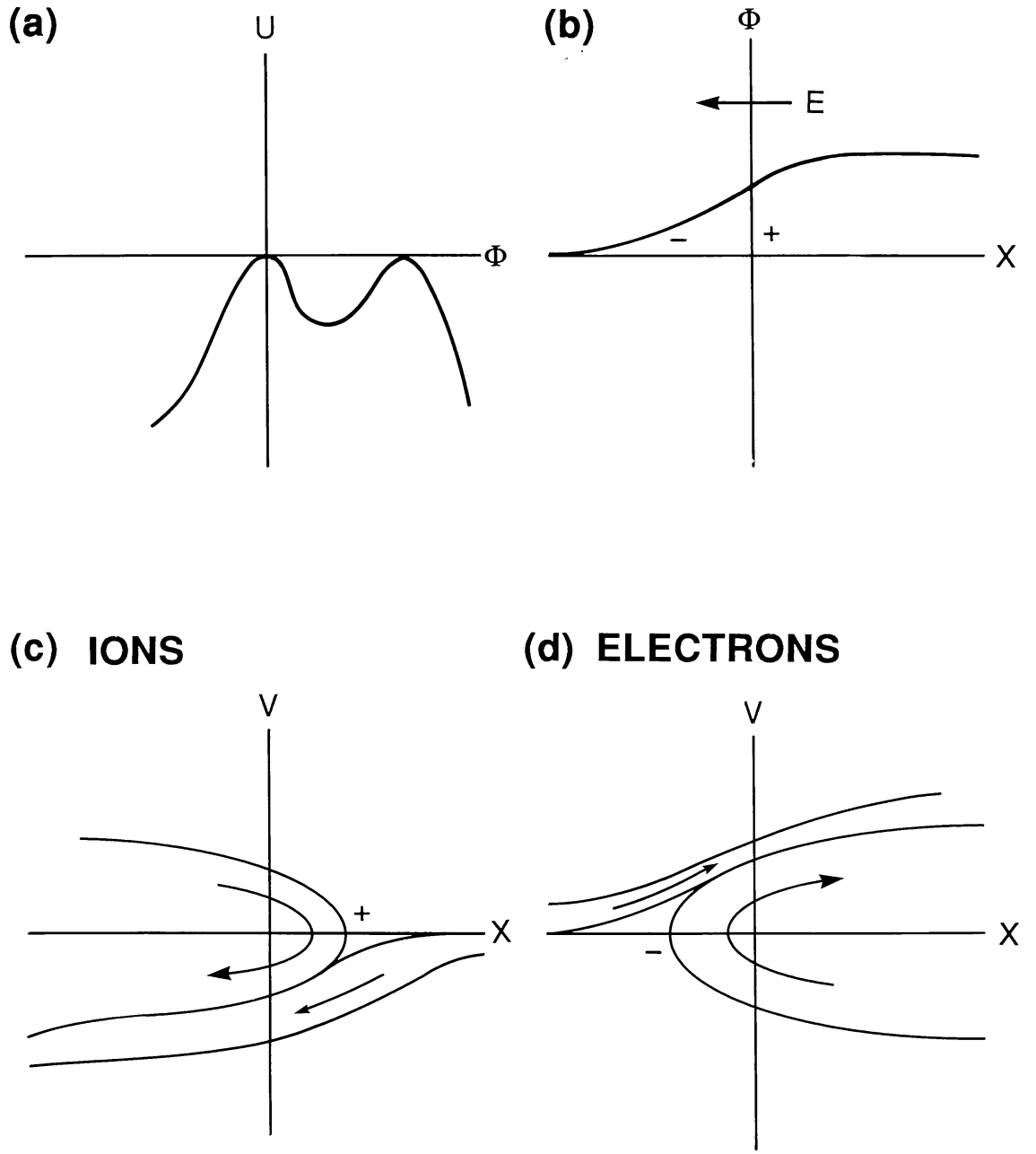

Fig. 5. (a) The effective potential for a plasma double layer. (b) The electrostatic potential for the classic double layer is a monotonic rise. Phase space plots for ions (c) and electrons (d) are also shown, with '+' and '−' signs indicating regions of net space charge.

a model with streaming electrons and ions and a hot population of electrons, it can be shown that the ion-drift velocity $u_0 > (T_e/m_i)^{1/2}$, the so-called Bohm criterion (Bohm, 1949; seel also Kan and Lee, 1980a; Hudson and Potter, 1981). One-dimensional unmagnetized BGK models of double layers are discussed by Block (1972, 1975), Knorr and Goertz (1974), Kan and Lee (1980a). While two-dimensional BGK solutions are difficult to find, structures perpendicular to the magnetic can be treated by considering a one-dimensional oblique model (Swift, 1975, 1979; Lotko and Kennel, 1981; Witt and Lotko, 1983; Witt and Hudson, 1986). Reviews of such models have been presented, e.g., by Goertz (1979) and Lee and Kan (1981).

While models of the BGK-type are useful in understanding the structure of double layers, they give no information at all as to the time-development of these structures. Plasma simulation can be used in order to determine the dynamics of double-layer formation. Early simulations (Goertz and Joyce, 1975; Hubbard and Joyce, 1979; Borovsky and Joyce, 1983) considered the two boundaries of the simulation to have a fixed potential difference between them, with $e\Phi/T_e \gg 1$, and found that the potential drop tended to concentrate in a double layer with a thickness of a few tens of Debye lengths. Such models are appropriate for simulation of laboratory double-layer experiments, but do not model the auroral situation very well since there are no grids that can be held at a fixed potential in space. Current-driven computer simulations (Sato and Okuda, 1981; Kindel *et al.*, 1981) have indicated that double layers can arise out of ion-acoustic turbulence driven by electron currents with drifts less than, but not too much less than, the electron thermal velocity. These double layers are characterized by potentials the order of the electron temperature ($e\Phi/T_e \approx 1$), widths the order of tens of Debye lengths, and lifetimes the order of hundreds of plasma periods. When much stronger currents are passed through a plasma, with drifts much greater than the electron thermal speed, a new regime of strong double layers associated with the Buneman instability with $e\Phi/T_e \gg 1$ can be found (Goertz and Joyce, 1975). Since such strong drifts are not very common in the auroral zone, and since auroral double layers are observed to have $e\Phi/T_e \approx 1$, we will concentrate on weak double layers in what follows.

Ion-acoustic double layers occur in a current carrying plasma as the result of the interaction of the electron current with an ion hole, which is a localized depletion of the ion density. In a normal, two-component plasma, it is well known that only a compressive ion-acoustic soliton can be formed. When additional components, such as a hot and cold electron component, are present, both compressive and rarefactive solitons can be formed (Lotko and Kennel, 1983). These modes, which propagate at the ion-acoustic speed, do not interact strongly with the ion population since in the ion-acoustic regime, $T_e \gg T_i$, the ion-acoustic speed is far out on the ion tail. On the other hand, it has been shown (Schamel, 1972; Bujurbarua and Schamel, 1981) that if trapped ions are included, a new ion hole mode can be formed with a speed the order of the ion thermal speed. Hudson *et al.* (1983) have shown that ion holes can exist in a plasma consisting of trapped and free-streaming ions and reflected and free-streaming electrons for a variety of plasma parameters. The Sagdeev potential and phase space for such an ion hole is depicted in Figure 6. As the amplitude of the ion hole grows, the barrier in the

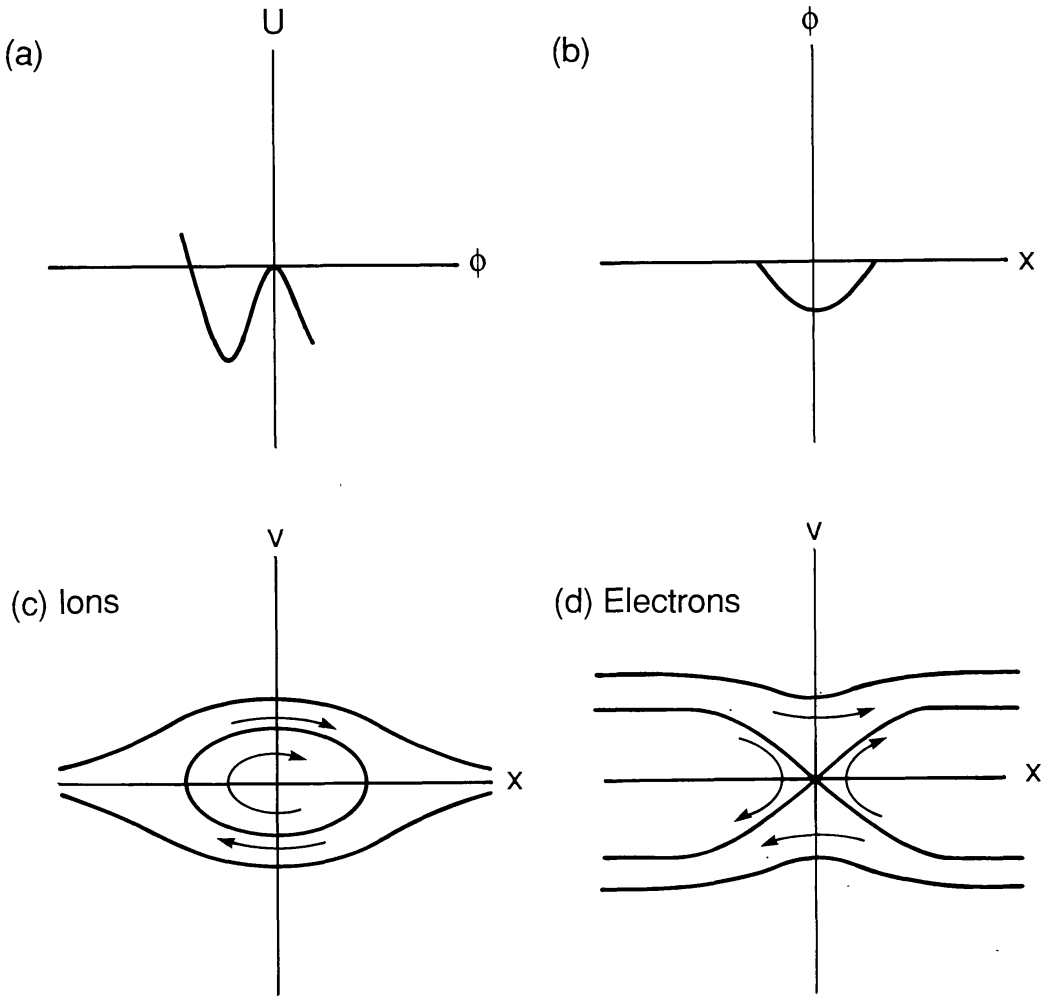

Fig. 6. Sagdeev potential (a), electrostatic potential (b), and ion (c) and electron (d) phase space diagrams for an ion hole. When the structure is in the presence of a current, more electrons are reflected from one side of the structure than the other, producing a double-layer potential as in Figure 4.

Sagdeev potential is lowered, and at some point the relative maximum for positive Φ becomes zero. At this point the effective potential looks like that in Figure 5, and the ion-hole solution becomes a double layer.

Particle simulations of ion-acoustic turbulence (Sato and Okuda, 1981; Barnes *et al.*, 1985) have shown that ion holes can form from ion-acoustic turbulence. As the hole grows, it slows down since it picks up more trapped ions. In the presence of a background current, the hole can grow rapidly into a double layer once its amplitude satisfies $e\Phi/T_e > m_e/m_i$ due to a process analogous to Landau damping known as reflection dissipation (Lotko, 1983). To understand this process, note that an ion hole, i.e., a negative potential dip, appears as a barrier to electrons (see Figure 6). If the electrons are drifting with respect to the hole, more electrons are approaching the hole and being reflected by it from the upstream side than from the downstream side. This leads to an enhancement of the electron density on the upstream side and a depletion on the downstream side so that the upstream side becomes negatively charged with respect to the downstream side and a net potential jump, i.e., a double layer, is formed

across the hole, with a potential structure like that in Figure 4. It is a necessary consequence of this scenario that the double layer is accompanied by a small negative potential dip.

The growth of ion holes was studied by Tetreault (1988) who showed that a nonlinear instability existed for drifts and temperature ratios below the linear stability threshold. When the ion and electron distribution functions have opposite slopes at a hole's velocity, the reflection dissipation mechanism described above causes the hole to slow down (in the ion frame) and thus to move to a velocity at which the unperturbed ion distribution function is larger. Since the hole maintains the value of its phase space density by Liouville's theorem, the relative magnitude of the hole becomes larger in this process. According to this model, thermal fluctuations can grow into holes for relative drifts of $V_D > 0.09 v_e$ (for $T_e = T_i$). As the amplitude of the hole grows, so does the nonlinear hole growth rate and so hole growth can be maintained for even weaker drifts.

While most work on double layers has concentrated on the one-dimensional structure of double layers, some computer simulations on two-dimensional ion-acoustic double layers have been performed (Barnes *et al.*, 1985). This work found that double layers would form if the plasma was strongly magnetized in the sense that $\Omega_e/\omega_{pe} > 1$, where Ω_e and ω_{pe} are the electron-cyclotron and plasma frequencies, respectively. In the weaker magnetic field regime, ion-acoustic turbulence was excited but it failed to organize itself into coherent double-layer structures. This is consistent with the observations of double layers, which appear always to occur in strong magnetic field regions of the auroral zone, at altitudes less than about 10 000 km. While the double-layer scale along the magnetic field was of the order of ten Debye lengths, as in one dimension, the transverse scale length of the double layers was the order of $10\sqrt{\lambda_D^2 + \rho_i^2}$. The double layers in this simulation were seen in conjunction with electrostatic ion-cyclotron turbulence, as in the spacecraft observations. Thus, it appears that while EIC waves can be excited by the same currents which support the double layers, the formation of the double layers themselves is associated more with ion-acoustic modes in contrast to the earlier anomalous resistivity models in which the parallel electric field is produced as a direct consequence of EIC turbulence.

A comparison of the effect of double layers and resistive potential drops on the overall current system was considered by Lysak and Hudson (1987). Parallel electric field models based on the EIC instability (Dum and Dupree, 1970; Lysak and Dum, 1983) and on the double-layer simulations (Barnes *et al.*, 1985) were introduced into an MHD model of auroral current flow to be described later in this review. Both models were successful at explaining the overall auroral potential drop, but differed in their effect on the global current system. In the resistive model, the current density becomes effectively reduced by magnetic diffusion which spreads the current over a larger area. On the other hand, the double-layer model the current could flow in a narrower current channel since adding additional current through a double layer increases the runaway population. Thus the double-layer model appears more capable of producing parallel potential drops on small spatial scales such as those in discrete arcs.

In light of these quite different models for the auroral parallel electric field, one might

ask about observational evidence for or against these models. As noted above, since the primary auroral beam is composed of runaway particles, it is difficult to assess the acceleration mechanism from these particles. One possible distinction relates to the location of the potential drop. Magnetic mirror supported electric fields scale with the magnetic mirror gradient, which is strongest at low altitudes. Thus the location of these fields is dependent on the point at which ionospheric particle populations begin to play an important role. In the models presented by Chiu and Schulz (1978), the peak electric fields were at 2000–3000 km altitude. In contrast, current-driven double layer or anomalous resistivity models have their peak parallel electric field at the point where the ratio of drift velocity to electron thermal velocity is largest, which occurs at altitudes of 5000–6000 km (Swift, 1978; Lysak and Hudson, 1979). Satellite observations indicate that ion beams are seen at altitudes above 5000 km (Ghielmetti *et al.*, 1978; Gorney *et al.*, 1981). Large transverse electric fields also appear to be correlated with parallel electric field signatures at altitudes above about 4500 km, but not below (Temerin *et al.*, 1981). An active experiment (Wilhelm *et al.*, 1985) has shown that 2–4 keV electrons emitted by a sounding rocket were reflected, presumably by a parallel electric field, at an altitude of 3000–4000 km. Finally, McFadden *et al.* (1987) observed time-varying electron fluxes with velocity dispersion indicating a source in the 4000–8000 km range. Thus, while these deductions are indirect, the indication is that the auroral acceleration region is primarily located in the region of about 1 R_E altitude, more consistent with current-driven mechanisms than with mirror supported potential drops.

4. Ionospheric Conductivity Effects

The field-aligned current systems discussed above must close perpendicular to the magnetic field through the ionosphere. In the ionosphere, ion collisions with atoms of the neutral atmosphere give rise to an anisotropic conductivity, with collisions in the *F*-layer where the collision frequency is comparable to the ion gyrofrequency giving rise to a Pedersen current in the direction of the electric field, while collisions in the *E*-layer where the ion-neutral collision frequency is much greater than the ion gyrofrequency giving rise to Hall currents in the $-\mathbf{E} \times \mathbf{B}$ direction (Rees, 1963; Hanson, 1965; Rishbeth and Garriott, 1969). The Pedersen conductivity is given by

$$\sigma_P = ne^2 \sum_s \frac{\nu_s/m_s}{\nu_s^2 + \Omega_s^2} , \tag{14}$$

where ν_s is the collision frequency of species s with the neutrals and Ω_s is the gyrofrequency. Typically in the ionosphere the electron collision frequency is much less than the gyrofrequency and so σ_P can be written as

$$\sigma_P = \frac{nec}{B}\left[\frac{\nu_i/\Omega_i}{1 + (\nu_i/\Omega_i)^2} + \frac{\nu_e}{\Omega_e}\right] \tag{15}$$

with the ion term dominating. The Hall conductivity can be written in general as

$$\sigma_H = -ne^2 \sum_s \frac{\Omega_s/m_s}{\nu_s^2 + \Omega_s^2} . \tag{16}$$

(Note here that the gyrofrequency has a sign, i.e., is negative for electrons.) Again in the limit $\nu_e/\Omega_e \ll 1$, the electron term becomes nec/B and the electron and ion terms can be combined to give

$$\sigma_H = \frac{nec}{B} \frac{1}{1 + (\Omega_i/\nu_i)^2} . \tag{17}$$

It can be seen that the Pedersen conductivity is largest for $\nu_i = \Omega_i$ while the Hall conductivity is largest for $\nu_i \to \infty$. We shall consider the effect of the ionospheric conductivity on the field-aligned current system, first considering steady-state effects and then considering the dynamics.

4.1. Steady-state ionosphere

For the purpose of considering the ionosphere's effect on the current systems of the magnetosphere, the ionosphere can be treated as a two-dimensional slab, and the Pedersen and Hall conductivities integrated over the ionospheric height. Then, in the rest frame of the neutral atmosphere, the total ionospheric current $\mathbf{I}$ can be given by:

$$\mathbf{I} = \boldsymbol{\Sigma} \cdot \mathbf{E} , \tag{18}$$

where

$$\boldsymbol{\Sigma} = \begin{bmatrix} \Sigma_P & -\Sigma_H \\ \Sigma_H & \Sigma_P \end{bmatrix},$$

where we have adopted the convention that the z-direction, and the direction of the background magnetic field, are in the downward direction. In the subsequent discussion, we will neglect the effect of neutral winds on the ionospheric currents, noting that the effects of such winds on the auroral current system were discussed by Lyons and Walterscheid (1986), and assume that Equation (18) holds in the rest frame of the Earth.

Since on long time-scales the plasma is quasi-neutral, the continuity of current requires that $\nabla \cdot \mathbf{j} = 0$. Integrating this equation over the ionospheric height, separating the equation into the parallel and perpendicular currents, and assuming that no field-aligned current escapes the bottom of the ionosphere, we can write

$$j_\parallel = \nabla \cdot \mathbf{I} = \nabla \cdot (\boldsymbol{\Sigma} \cdot \mathbf{E}) , \tag{19}$$

where Equation (18) has been used in the last equality. Note again that $j_\parallel$ is the current entering the ionosphere from above and is positive for downward current and negative for upward current. It should be noted that, strictly speaking, the left-hand side of Equation (19) should be corrected for the fact that the geomagnetic field line is not

vertical, and written as $j_\parallel \sin I$ where I is the inclination angle of the magnetic field. Since $I \geq 65°$ for auroral field lines, neglect of this factor is less than a 10% error. For simplicity, we shall neglect the inclination angle in the discussion to follow.

Breaking the conductivity tensor into Pedersen and Hall terms and writing the electric field as $\mathbf{E} = -\nabla\Phi_I$, we have

$$j_\parallel = -(\Sigma_P \nabla^2 \Phi_I + \nabla\Sigma_P \cdot \nabla\Phi_I - \nabla\Sigma_H \times \nabla\Phi_I \cdot \hat{\mathbf{z}}) . \tag{20}$$

Therefore, if the conductivities are uniform, only the Pedersen currents can close the field-aligned currents. In this situation, the Hall currents are source-free and thus form closed loops. It can be shown (Dungey, 1963; Hughes, 1974) that the ground magnetic perturbation in this case is solely due to these Hall currents; the contributions from the Pedersen and field-aligned currents cancel for a localized perturbation.

If we assume constant conductivities, we can combine Equation (20) with the linear current-voltage relation (6) which we rewrite, defining $\Delta\Phi = \Phi_I - \Phi_0$, where Φ_0 is the potential in the source, as:

$$j_\parallel = -K(\Phi_I - \Phi_0) . \tag{21}$$

Eliminating the field-aligned current from (20) and (21), we arrive at an equation for the ionospheric potential in terms of the source potential:

$$\left[1 - \frac{\Sigma_P}{K} \nabla^2\right] \Phi_I = \Phi_0 . \tag{22}$$

If we consider the Fourier decomposition of the source potential, we can write

$$\Phi_{Ik} = \frac{\Phi_{0k}}{1 + k^2 L^2} , \tag{23}$$

where the scale length $L = \sqrt{\Sigma_P / K}$. For typical auroral parameters of $\Sigma_P = 10$ mho and $K = 1$ nanomho m^{-2}, the scale length $L = 100$ km. The parallel potential drop is then given by

$$\Delta\Phi_k = -\Phi_{0k} \frac{k^2 L^2}{1 + k^2 L^2} \tag{24}$$

indicatig that potential structures with a scale smaller than L will lead to a potential drop, while larger scale structures will not.

An experimental tet of this model was performed using Dynamics Explorer data by Weimer *et al.* (1985) who found that to lowest order the data taken at two different altitudes on approximately the same field line supported the model given above. It is interesting to note that these authors found that the effective conductance K was the same for upward and downward currents. This observation is consistent with the anomalous resistivity model but not with the adiabatic model in which upward currents carried by plasma sheet electrons should require a larger potential drop than downward currents carried by ionospheric electrons.

While the assumption of uniform conductivity may be reasonable on the local scale, strong gradients of the conductivity exist because of the day-night asymmetry of solar radiation, and because of the enhancement of conductivity in the auroral oval due to precipitation. Detailed empirical models of the conductivity distribution have been given by Wallis and Budzinski (1981), Vickrey *et al.* (1981), and Spiro *et al.* (1982) and were summarized by Reiff (1984).

These gradients can have observable effects on the convection pattern over the polar cap. Atkinson and Hutchinson (1978) considered the convection pattern produced due to an exponential profile of conductivity, with a fixed potential assumed on the boundary of the polar cap. They found that the effect of the day-night gradient was to break the dawn-dusk symmetry of the convection pattern, producing more intense convection on the dawn side of the polar cap and the dusk side of the auroral zone.

Yasuhara *et al.* (1983; see also Vasyliunas, 1970) considered the effect of the auroral conductivity ridge, under conditions of a fixed current distribution. It was found in this study that the convection pattern was rotated clockwise (when looked at from above in the northern hemisphere) such that the boundary between flow lines which close in the dusk and dawn auroral zones was rotated toward the afternoon on the dayside and the post-midnight sector at night. These effects have impact on efforts to model the dependence of the convection pattern on the interplanetary field, since rotations of the convection pattern are also thought to occur as the result of the variation of the B_y (dawn-to-dusk) component of the interplanetary magnetic field (e.g., Heppner, 1972; Heelis *et al.*, 1976, 1983; Reiff *et al.*, 1978; Burch *et al.*, 1985; Moses *et al.*, 1987).

4.2. Ionospheric Dynamics

Although the solar input to the ionosphere is only slowly changing, the input due to precipitation can vary quite rapidly. This enhanced ionization can feed back on the auroral current systems since the resulting gradients in the conductivities can feed field-aligned currents (cf. Equation (20)). As can be seen from Equations (14)–(17), the conductivity is simply proportional to the density if the ion-neutral collision frequency is constant. Since the ion-neutral collision frequency depends only on the neutral density (Rishbeth and Garriott, 1969), it may in fact be assumed to be roughly constant in time, and the conductivities may be considered to be proportional to the plasma density.

We can write the ionospheric continuity equation in the form:

$$\frac{\partial n}{\partial t} + \nabla \cdot (n\mathbf{v}) = S - \alpha(n^2 - n_0^2)\,, \tag{25}$$

where S is the source term due to precipitation, α is the recombination coefficient, and n_0 is the plasma density produced by solar illumination. The recombination coefficient $\alpha \approx 10^{-7}\,\mathrm{cm^3\,s^{-1}}$ is primarily due to dissociative recombination (Rishbeth and Garriott, 1969). The source term S depends on the flux and energy of the precipitating electrons, and was shown by Rees (1963) to be proportional to the input energy flux, times a function which depends upon the composition of the neutral atmosphere and

location at which the energy is deposited. This model gives a source term integrated over the ionospheric height of approximately $Sh = \varepsilon/(35\text{ eV})$ (see also Coroniti and Kennel, 1972), where ε is the precipitating energy flux in ergs $\text{cm}^{-2}\ \text{s}^{-1}$. Note that in the uniform steady state the density can be given by

$$n = \sqrt{n_0^2 + S/\alpha} \tag{26}$$

and so when the precipitation source dominates, the density should be proportional to the square root of the input energy flux.

To convert the densities to height-integrated conductivities, we must multiply by the appropriate factors (Equations (14)–(17)), and integrate over the ionospheric height. We can summarize such operations by writing $\Sigma_P = Pn$ and $\Sigma_H = Hn$. Then the continuity equation for the Pedersen conductivity can be written:

$$\frac{d\Sigma_P}{dt} = S_P - \alpha_P(\Sigma_P^2 - \Sigma_{P0}^2)\,, \tag{27}$$

where d/dt is the convective derivative, $S_P = SP$ is the source for the conductivity, and $\alpha_P = \alpha/P$ is the recombination coefficient. An equation similar to (27) can be written for the Hall conductivity. Various models for these coefficients have deduced empirically (Harel *et al.*, 1981; Wallis and Budzinski, 1981; Vickrey *et al.*, 1981; Spiro *et al.*, 1982; Reiff, 1984). Harel *et al.* (1981) have written the contribution of the Pedersen conductivity due to precipitation as $\Sigma_P = 5.2\text{ mho}\ \varepsilon^{1/2}$, and the Hall conductivity as $\Sigma_H = 0.55W^{0.66}\Sigma_P$, where W is the energy of the incident electrons. The energy dependence of the Hall conductivity can be qualitatively explained by noting that more energetic particles deposit their energy at lower altitudes where the Hall currents flow. Spiro *et al.* (1982), attempting to fit the data of Vickrey *et al.* (1981) have modified these relations as

$$\Sigma_P = \frac{20W}{4 + W^2}\,\varepsilon^{1/2}\,, \tag{28}$$

$$\Sigma_H = W^{5/8}\Sigma_P\,. \tag{29}$$

In the present notation, these relations imply that $H/P = W^{5/8}$ and that the Pedersen source term S_P *is*

$$S_P = \frac{\alpha}{P}\left[\frac{20W}{4 + W^2}\right]^2 \varepsilon\,. \tag{30}$$

For $\alpha = 3 \times 10^{-7}\ \text{cm}^3\ \text{s}^{-1}$ and $P = 3 \times 10^{-5}\ \text{mho cm}^3$, we have $S_P = 0.16\ \text{mho s}^{-1}\ \varepsilon$ for $W = 1$ keV.

Lyons (1980) has considered the response of the auroral flux tube to an assumed source potential in the outer magnetosphere, using the linear current-voltage relation and the conductivity model of Harel *et al.* (1981). It was found, as would be expected from Equation (22), that the sharp features of the assumed source potential were smoothed

out by this ionospheric filtering effect. The self-consistency of the model was checked by comparison with rocket flights by determining the high-altitude potential distribution from the observed energy of precipitating electrons and the observed ionospheric electric fields. This inferred high-altitude potential was then used as input to the model equations, which were then used to solve for the ionospheric potential. The agreement here was reasonably good. Kan and Lee (1980b) presented a similar model, in which the deceleration of the assumed convection in the outer magnetosphere was taken into account.

A more detailed model of this type was presented by Chiu and Cornwall (1980), who considered deviations from quasi-neutrality by using a Poisson's equation in two dimensions, including the low-frequency transvese dielectric constant $\varepsilon = 1 + c^2/V_A^2$, where V_A is the Alfvén speed (cf. Swift, 1975). The densities in Poisson's equation were determined by the particle populations as in Chiu and Schulz (1978), and the system of equations was closed by using the linear current-voltage relation (6) and the ionospheric Equations (20) and the steady-state limit of (25). The ionospheric source term was taken to be proportional to the incoming current, rather than the energy flux (see also Atkinson, 1970; Sato, 1978). This set of equations was solved iteratively, with the starting point being observed particle populations. Solutions exhibiting the reversed electric field signatures typical of the S3-3 observations (Mozer *et al.*, 1977, 1980) were found, with the scale length being given by a modified ionospheric scale length $L = \sqrt{(\frac{2}{3})\Sigma_P/K}$. This work was extended by the work of Chiu *et al.* (1981) who considered the return current region by allowing the field-aligned conductance density K to be position-dependent, and by Newman *et al.* (1986) who investigated the effect of this two-dimensional model on the auroral plasma populations.

5. Time-Dependent Coupling

The steady-state model discussed above can give a reasonable description of the structure of auroral currents; however, it is difficult to generalize this model to time-dependent situations. While observations often show a rather steady auroral current pattern, in a wide class of events, including the passage of flux transfer events, substorm phenomena such as the westward traveling surge, and in cases where the ionospheric conductivity is varying in time, a steady-state model is not appropriate. In such cases, it is useful to consider the plasma as a magnetized fluid, and describe the dynamics using the equations of magnetohydrodynamics (MHD), which represent the conservation laws for mass, momentum and energy combined with Maxwell's equations. The basic equations for a MHD fluid are:

$$\frac{\partial \rho}{\partial t} + \nabla \cdot (\rho \mathbf{v}) = 0 \,, \tag{31}$$

$$\rho \frac{\mathrm{d}\mathbf{v}}{\mathrm{d}t} = -\nabla p + \frac{1}{c}\,\mathbf{j} \times \mathbf{B} + \nu \nabla^2 \mathbf{v} \,, \tag{32}$$

$$\rho c_v T \frac{\mathrm{d}}{\mathrm{d}t} \log \frac{p}{\rho^\gamma} = \mathbf{j} \cdot \mathbf{E} - \nabla \cdot \mathbf{q}\,, \tag{33}$$

where ρ is the mass density, t is the time, $\mathbf{v}$ is the fluid velocity, p is the pressure, $\mathbf{j}$ is the current density, $\mathbf{B}$ is the magnetic field, ν is the viscosity, c_v is the specific heat, T is the temperature, and $\mathbf{q}$ is the heat flux. In these equations the convective derivative, $\mathrm{d}/\mathrm{d}t \equiv \partial/\partial t + \mathbf{v} \cdot \nabla$ is used. These equations are supplemented with Maxwell's equations and the generalized Ohm's Law:

$$\mathbf{E} + \frac{1}{c}\,\mathbf{v} \times \mathbf{B} = \frac{\mathbf{j}}{\sigma} + \frac{m_e}{ne^2}\left[\frac{\partial \mathbf{j}}{\partial t} + \nabla \cdot (\mathbf{j}\mathbf{v} + \mathbf{v}\mathbf{j})\right] - \frac{1}{ne}\,\nabla \cdot \mathbf{P} + \frac{1}{nec}\,\mathbf{j} \times \mathbf{B} \tag{34}$$

in which c is the speed of light, σ is the conductivity, e and m_e are the electronic charge and mass, and n is the particle density. In cases where the scale lengths are large, all of the terms on the right-hand side except the first are zero. The other terms represent inertial effects, pressure (finite beta) effects, and the Hall effect, respectively. In the case where the entire right-hand side is zero, we have the 'frozen-in' condition, in which the electric field is simply given by $\mathbf{E} = -\mathbf{v} \times \mathbf{B}/c$, or equivalently, the plasma flows at a velocity given by $\mathbf{v} = c\mathbf{E} \times \mathbf{B}/B^2$. On the other hand, if resistivity is important, the current density may be given by $\mathbf{j} = \sigma(\mathbf{E} + \mathbf{v} \times \mathbf{B}/c)$. In addition, when the time and spatial scales are large, we may assume that the fluid is quasi-neutral and that the displacement current is negligible. Under these assumptions, Maxwell's equations and the generalized Ohm's Law can be combined into the induction equation

$$\frac{\partial \mathbf{B}}{\partial t} = \nabla \times (\mathbf{v} \times \mathbf{B}) + \eta \nabla^2 \mathbf{B}\,, \tag{35}$$

where $\eta = c^2/4\pi\sigma$ is the magnetic diffusivity.

5.1. Alfvén wave propagation

The auroral plasma is, to lowest approximation, cold in the sense that the plasma pressure is much less than the magnetic field pressure (i.e., $\beta = 8\pi p/B^2 \ll 1$), and so the heat equation (33) can be neglected. In addition, the plasma is collisionless, so the viscosity and the magnetic diffusivity are nearly zero. It is well known (e.g., Kantrowitz and Petschek, 1966) that such an ideal MHD fluid supports three wave modes, the fast (or magnetosonic), slow, and intermediate, or Alfvén, waves. Changes in the field-aligned current are associated with the passage of the Alfvén wave. Such a wave can be described to lowest order by the ideal MHD equations, in the case where the wave propagation is totally allong the background magnetic field. In this case we can rewrite the MHD equations as:

$$\rho \frac{\partial \mathbf{v}}{\partial t} = \frac{\mathbf{j} \times \mathbf{B}}{c} = \frac{1}{4\pi} B_0 \frac{\partial \mathbf{b}}{\partial z}\,, \tag{36}$$

$$\frac{\partial \mathbf{b}}{\partial t} = \nabla \times (\mathbf{v} \times \mathbf{B}) = B_0 \frac{\partial \mathbf{v}}{\partial z}\,, \tag{37}$$

where the background magnetic field B_0 is assumed to be in the z-direction and $\mathbf{b}$ is the magnetic perturbation. Linearization of Equations (36) and (37) indicates that the wave travels at the Alfvén speed $V_A = B_0/\sqrt{4\pi\rho}$ and that the fluid velocity is related to the magnetic field perturbation by $\mathbf{v} = \pm \mathbf{b}/\sqrt{4\pi\rho}$.

This wave can be looked upon in another way by considering the relationship between the electric fields and the currents. The perpendicular electric field associated with the wave can be found by the frozen-in condition:

$$\mathbf{E}_\perp = -\frac{\mathbf{v} \times \mathbf{B}_0}{c} = \pm \frac{\mathbf{B}_0 \times \mathbf{b}}{c\sqrt{4\pi\rho}} \tag{38}$$

and the perpendicular current can be calculated from Ampère's Law:

$$\mathbf{j}_\perp = \frac{c}{4\pi} \nabla \times \mathbf{b} = \frac{c}{4\pi} \frac{\partial \mathbf{b}}{\partial z} . \tag{39}$$

Combining these two equations and defining the current intensity $\mathbf{I}_\perp = \int dz \mathbf{j}_\perp$, we can write the relation between current and electric fields as an Ohm's Law:

$$\mathbf{I}_\perp = \pm \frac{c^2}{4\pi V_A} \mathbf{E}_\perp . \tag{40}$$

This equation may be compared with the ionospheric Ohm's Law in the presence of a Pedersen conductivity $\mathbf{I}_\perp = \Sigma_P \mathbf{E}_\perp$. This analogy leads to the definition of the wave conductivity, or Alfvén conductivity $\Sigma_A = c^2/4\pi V_A$. (Strictly speaking, Σ_A should be considered to be an admittance, rather than a conductivity, since it does not imply any Ohmic dissipation. However, in what follows we shall be a little sloppy with notation and refer to Σ_A as an Alfvén wave conductivity.)

This similarity betwee the ionospheric and Alfvén wave relationships makes it somewhat difficult to distinguish between static current patterns closing by a Pedersen current and propagating Alfvén waves. In both cases, the ratio between measured electric and magnetic perturbations can be written as $E/B = c/4\pi\Sigma$, where Σ is Σ_P or Σ_A, respectively, for the steady-state and Alfvén wave cases. The main way in which the two models can be distinguished is the fact that the Pedersen conductivity is generally greater than 1 mho while Alfvén conductivities are typically 0.1 mho or less (see Figure 7). Sugiura *et al.* (1982) have made observations supporting the steady-state mechanism, finding conductivities ranging from 2 to 10 mhos from low altitudes. On the other hand, Gurnett *et al.* (1984) have done a similar measurement from the higher altitude DE-1 and have noted that the effective conductivity appears to decrease with increasing radial distance, tentatively supporting the Alfvén wave model. Effective conductivities observed were the order of 1 mho.

The large difference between the Alfvén and Pedersen conductivities leads to a reflection of Alfvén waves when they reach the ionosphere. A boundary value calculation may be done in which the currents associated with incident and reflected Alfvén

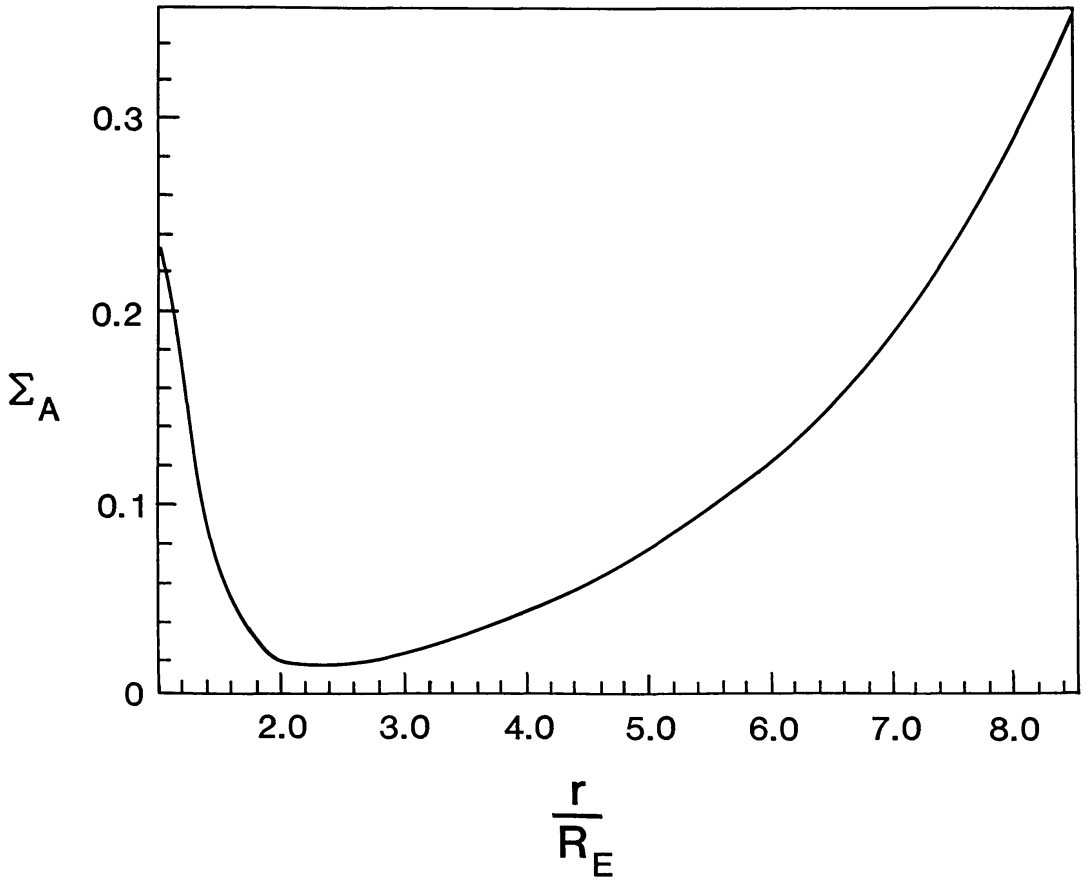

Fig. 7. Plot of the effective Alfvén admittance Σ_A (in mho) as a function of altitude along an auroral field line for a dipole magnetic field at invariant latitude 70° and a density profile given by $n(r) = 10^5\, e^{-(r-r_0)/h} + 5(r-1)^{-1.5}$, where r is in R_E, $r_0 = 1.05\, R_E$ andn $h = 0.1\, R_E$ (from Lysak and Hudson, 1987).

waves are matched with the ionospheric currents. It is then found that the reflection coefficient for the wave defined as $R = E_{\text{ref}}/E_{\text{inc}}$, is given by (Mallinckrodt and Carlson, 1978):

$$T = \frac{\Sigma_A - \Sigma_P}{\Sigma_A + \Sigma_P} \,. \tag{41}$$

Therefore, in the usual situation where $\Sigma_A < \Sigma_P$, the reflected wave has an electric field in the opposite direction as the incident electric field. Thus the resistance of the ionosphere is transmitted to the outer magnetosphere by the reflected wave which tends to decrease the perpendicular electric field and thus the convection velocity. Reflections of Alfvén waves occur also in situations where the conductivity is non-uniform and where Hall currents are important. This situation has been considered by Ellis and Southwood (1983) and Glassmeier (1983, 1984).

It should be noted that the simple relationship between E and B as given above can break down when incident and reflected waves interfere with each other. Figure 8 shows results from a numerical calculation in which a source region for Alfvén waves is moving with respect to the plasma (Lysak, 1985). There are two noteworthy features of this run.

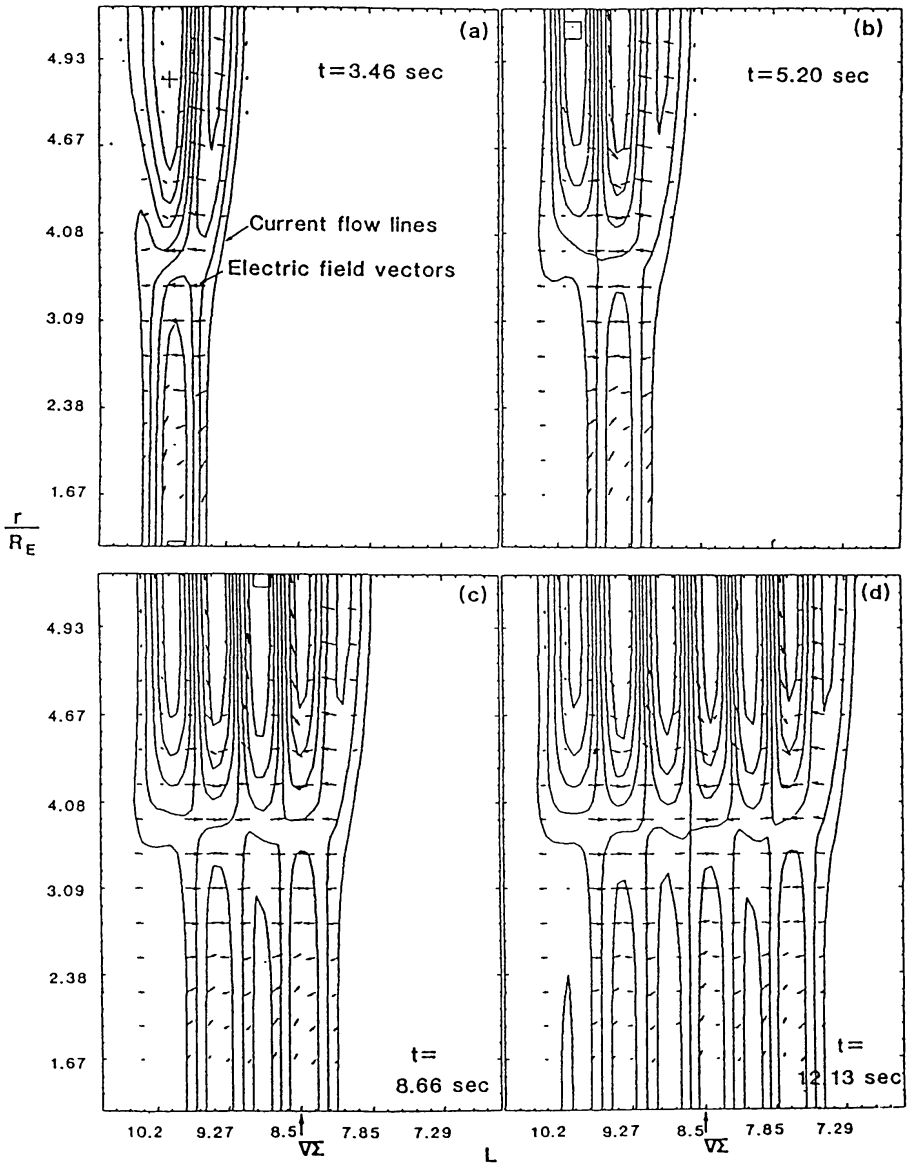

Fig. 8. Results of a numerical model of magnetosphere-ionosphere coupling (Lysak, 1985) in which a pulse has been moved across the system. Reflections of Alfvén waves cause an interference region to be set up which causes some of the inospheric currents to close before reaching high altitudes. In the interference region, the electric and magnetic fields become 90° out of phase (not shown).

First, the currents which close in the ionosphere do not extend all the way to the source in this case, but instead close in the interference region, which is between 3 and 4 R_E in this case. In addition, the electric and magnetic fields are directly correlated as indicated above in the leading pulse, but become 90 degrees out of phase in later pulses when up and downgoing waves interfere. Thus it would be expected that such standing wave structures should be observed in active auroral regions where moving current systems are likely.

The ideal MHD picture of the Alfvén waves breaks down when the wavelength perpendicular to the background magnetic field becomes small. For cold plasmas such as those at lower altitudes, where the electron thermal speed v_e is less than the Alfvén

speed, the corrections are due to the inertial term in the generalized Ohm's Law and so the electron inertial length c/ω_{pe} is the relevant scale length. In this regime the wave dispersion relation becomes (Goertz and Boswell, 1979):

$$\omega = \frac{k_{\parallel} V_A}{\sqrt{1 + k_{\perp}^2 c^2/\omega_{pe}^2}} \,. \tag{42}$$

On the other hand, at higher altitudes where $v_e > V_A$, kinetic effects (finite ion-Larmor radius) become important and the dispersion relation becomes (Hasegawa, 1976):

$$\omega = k_{\parallel} V_A \sqrt{1 + k_{\perp}^2 \rho^2} \,, \tag{43}$$

where $\rho = \rho_i \sqrt{T_e/T_i + \frac{3}{4}}$ is a gyroradius based on a combination of the electron and ion temperatures. Both of these regimes have been termed the kinetic Alfvén wave, although strictly speaking the name is applicable only to the dispersion relation (43).

The significant difference between these kinetic Alfvén waves and the ideal MHD Alfvén wave is that the kinetic waves carry a parallel electric field, which can be given by

$$E_{\parallel} = - \frac{c^2/\omega_{pe}^2}{1 + k^2 c^2/\omega_{pe}^2} \frac{\partial}{\partial z} \nabla \cdot \mathbf{E}_{\perp} \tag{44}$$

in the inertial limit and

$$E_{\parallel} = \rho^2 \frac{\partial}{\partial z} \nabla \cdot \mathbf{E}_{\perp} \tag{45}$$

in the kinetic limit. Note that the parallel electric field has opposite sign in the two limits. In the inertial case, the electrons must be accelerated in order to carry the required field-aligned current, and $j_{\parallel} E_{\parallel} > 0$. On the other hand, electrons are decelerated in the kinetic wave and $j_{\parallel} E_{\parallel} < 0$.

The existence of the parallel electric field in the kinetic Alfvén wave indicates that this wave can have a Landau resonance with electrons. In the kinetic limit, Hasegawa and Mima (1978) have shown that these waves can be responsible for plasma diffusion, anomalous resistivity and electron heating. Goertz and Boswell (1979) have noted that successive passages of a kinetic Alfvén wave can accelerate ion beams. Lysak and Carlson (1981) showed that in the inertial regime, the electron population is accelerated in bulk, producing a drifting population that could become unstable to current-driven instabilities. It should be noted that the parallel fields given by (44) and (45) are transient fields, and disappear in the steady state. The excitation of instabilities by the current in these waves can lead to the formation of a steady electric field through the formation of double layers or anomalous resistivity.

The propagation of kinetic Alfvén waves through a region of parallel electric fields was considered by Lysak and Carlson (1981) and modeled numerically by Lysak and Dum (1983). In the linear regime, the effective resistivity in a parallel electric field region can modify the Alfvén wave dispersion relation, leading to a reflection and absorption

of these waves. These reflections are of an opposite sense as the ionospheric reflections described by Equation (41), i.e., the perpendicular electric field of the reflected wave is in the same direction as the incident wave. Thus reflections from a parallel electric field region can lead to intensifications of the perpendicular electric field, leading to the formation of the large electric fields observed by S3-3 and other satellites. The reflection efficiency is also dependent on the transverse wave number of the Alfvén wave, with short wavelength waves being reflected and long wavelength waves transmitted. At intermediate wave numbers, the absorption of the wave reaches a maximum (Lysak and Dum, 1983).

These wave reflection characteristics have important consequences for the coupling of the magnetospheric convection to the ionosphere. For large-scale structures, the Alfvén waves are transmitted through the parallel electric field region and reflect from the ionosphere, allowing the ionospheric drag to be transmitted to the outer magnetosphere. On the other hand, small-scale structures are reflected from the $E_{\parallel}$ region and so the magnetosphere is effectively cut off from the ionosphere. Lysak and Dum (1983) also showed that increasing the current density, and thus the strength of the parallel electric field, at a fixed scale size led to an increasing decoupling of the ionosphere and magnetosphere. After a few Alfvén bounce times, an electrostatic structure consistent with the S3-3 observations of Mozer *et al.* (1977, 1980) is set up. Thus the so-called 'electrostatic shocks' are in a sense neither shocks nor electrostatic, but rather the result of a dissipative, electromagnetic system.

5.2. Ionospheric feedback

Time-varying auroral currents such as those discussed above can give rise to time variations in the ionospheric conductivity as mentioned in Section 4.2. This leads to the possibility of a feedback interaction between the ionospheric dynamics and the propagation of Alfvén waves along auroral field lines. Such interactions may be responsible for the propagation of auroral arc structures (Sato, 1978; Miura and Sato, 1980; Watanabe and Sato, 1988) and also possibly for the propagation of the westward traveling surge (Akasofu *et al.*, 1965; Kisabeth and Rostoker, 1973; Opgenoorth *et al.*, 1980, 1983; Inhester *et al.*, 1981; Rothwell *et al.*, 1984, 1988; Kan *et al.*, 1984).

Consider an enhancement in the ionospheric conductivity in the presence of a background current, as is indicated in Figure 9. Current continuity requires either that the current is enhanced in the conductivity bump, or that the driving electric field is modified by polarization charges building up on the sides of the bump. If the current is enhanced, field-aligned currents must flow at the gradients in the ionospheric conductivity, as is indicated by Equation (20). The precipitation associated with the upward currents can lead to enhanced ionization, while recombination proceeds on the side on which downward currents flow. The net result is that the conductivity enhancement can propagate in the direction of the background current. The degree to which this can occur depends on the efficiency with which the conductivity enhancements can be polarized. As we shall see below, this depends on the response of the magnetosphere to this new field-aligned current.

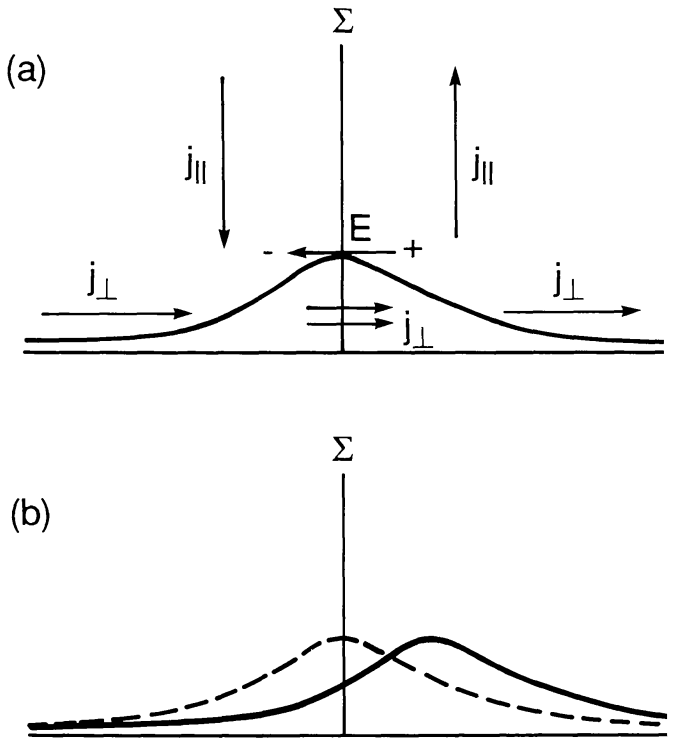

Fig. 9. Schematic illustration of the ionospheric feedback mechanism. (a) When a conductivity enhancement exists in the presence of a background current, charges build up on each side of the enhancement, either producing a reversed electric field, or leading to an increased current through the bump which closes via field-aligned currents. (b) When the upward current is carried by precipitating hot electrons, the conductivity bump moves in the direction of the current since ionization is created by the precipitating electrons, while recombination occurs on the trailing edge.

Sato (1978) has analyzed this instability by linearizing the continuity equation (25) and writing the source term S as $S = -Qj_{\parallel}$. Characterizing the magnetospheric response by an impedance Z:

$$\nabla^2 \Phi = Z j_{\parallel} , \tag{46}$$

we can eliminate the field-aligned current from (20) and (46) and write

$$\nabla^2 \Phi_I = -\frac{Z}{1 + Z\Sigma_P} \left[P \nabla n \cdot \nabla \Phi_I + H \nabla \Phi_I \times \nabla n \cdot \hat{\mathbf{z}} \right] . \tag{47}$$

Rewriting (25) with the source $S = -Qj_{\parallel}$, using (46) to eliminate the field-aligned current, and letting the velocity be the $\mathbf{E} \times \mathbf{B}$ drift, we have

$$\frac{\partial n}{\partial t} = \frac{QP}{1 + Z\Sigma_P} \nabla n \cdot \nabla \Phi_I + \left[\frac{c}{B} - \frac{QH}{1 + Z\Sigma_P} \right] \nabla n \times \nabla \Phi_I \cdot \hat{\mathbf{z}} . \tag{48}$$

Linearization of Equations (47) and (48) about an equilibrium density n_0 and a background electric field $\mathbf{E}_0$ yields a dispersion relation:

$$\omega = \mathbf{k} \cdot \mathbf{v}_0 + \frac{Q(\mathbf{k} \times \hat{\mathbf{z}} H + \mathbf{k} P) \cdot \mathbf{E}_0}{1 + Z\Sigma_{P0}} - 2i\alpha n_0 , \tag{49}$$

where $\mathbf{v}_0 = c\mathbf{E}_0 \times \hat{\mathbf{z}}/B_0$. Note that when the numerator of the second term is positive (negative) and the imaginary part of Z is negative (positive), the imaginary part of ω can be positive, leading to instability, if the growth is larger than the damping due to recombination. In addition, when the gradients are parallel to the electric field direction, the Pedersen currents drive the instability, while for gradients perpendicular to $\mathbf{E}$ the Hall curents are destabilizing.

In order to determine the magnetospheric impedance Z, we must consider the response of the magnetosphere to an Alfvén wave launched from the ionosphere. In the magnetosphere, the field-aligned current density can be related to the electric fields by the Alfvén conductivity Σ_A defined by Equation (40):

$$j_{\parallel} = \pm \Sigma_A \nabla \cdot \mathbf{E}\,, \tag{50}$$

where the plus (minus) sign is for downgoing (upgoing) waves. Let the wave launched by the ionosphere be reflected in the magnetosphere such that the current in the reflected wave is the same (or opposite) in sign to the incident wave, $j_{\parallel}^{\text{ref}} = \pm j_{\parallel}^{\text{inc}}$. (We will see in the next section that these conditions correspond to voltage, and current generators, respectively.) If T represents the travel time of the wave from the ionosphere to the reflection point, there will be a phase lag of $2\omega T$ between the time the incident wave is launched and the time the reflected wave returns to the ionosphere. Thus we have

$$j_{\parallel I}^{\text{ref}} = \pm e^{2i\omega T} j_{\parallel \text{I}}^{\text{inc}} \tag{51}$$

and the electric fields will have a similar relation with opposite sign. Now noting that Equation (46) holds for the superposition of the incident and reflected waves, we can use (50) to write

$$j_{\parallel I}^{\text{ref}} = \frac{1 - Z\Sigma_A}{1 + Z\Sigma_A}\, j_{\parallel I}^{\text{inc}}\,. \tag{52}$$

Comparing (51) and (52), we find that in the voltage generator case, we have $Z = i\cot(2\omega T)/\Sigma_A$ and in the current generator case $Z = -i\tan(2\omega T)/\Sigma_A$. Thus instability occurs when the current in the reflected wave lags the incident current, while for a current generator, the reflected current must lead the incident current for instability.

Miua and Sato (1980), Kan and Sun (1985), and Watanabe and Sato (1988) have performed simulations of the feedback as applied to global auroral arc formation. In the work of Miura and Sato (1980), a lumped circuit description of the magnetospheric response was assumed, as in the work of Sato (1978), and the two-dimensional ionosphere was modeled. Kan and Sun (1985) improved on this model by taking account of the finite Alfvén wave travel time between the ionosphere and the equatorial plane. This model was able to address the excitation of Pi2 pulsations (cf. Southwood and Hughes, 1983; Baumjohann and Glassmeier, 1984). Watanabe and Sato (1988) performed a three-dimensional simulation in which, however, the Alfvén speed was assumed to be constant along a field line. This work produced results similar to those of Kan and Sun (1985).

As opposed to these global models, the feedback instability has been applied to the propagation of the westward traveling surge by Rothwell *et al.* (1984, 1986, 1988). They introduced a closure parameter α which measures the strength of the field-aligned currents flowing at the boundaries of the ionization enhancement behind the surge, with $\alpha = 0$ implying no field-aligned current (total polarization) and $\alpha = 1$ implying total closure by the field-aligned current. This parameter is related to the magnetospheric impedance defined above by $\alpha = 1/(1 + Z\Sigma_P)$ (Lysak, 1986). A similar parameter was introduced by Kan *et al.* (1984), but in this work the motion of the surge was not related to the feedback instability but rather to the propagation of ion-acoustic waves. Rothwell *et al.* (1984) showed that the speed of the surge was proportional to α, a result simila to that presented above in Equation (49). In addition, the propagation direction of the surge was related to α, with purely westward propagation occurring for $\alpha = 0$ with the direction turning northward for finite α. Eastward propagation was even possible for the case of overclosure $\alpha > 1$, which may be related to the Viking observation that 'surges' may be stationary or even propagate eastward as well as westward (Rostoker *et al.*, 1987).

The westward traveling surge has been associated with micropulsations in the Pi2 band (Rostoker and Samson, 1981; Pashin *et al.*, 1982; Samson and Rostoker, 1983; Baumjohann and Glassmeier, 1984) as well as higher frequency PiB pulsations (Opgenoorth *et al.*, 1980). It is thought that these pulsations are the result of an Alfvén wave impulse which damps as it reflects off the ionosphere (Maltsev *et al.*, 1974), with the wave frequency determined by the bounce time of Alfvén waves between conjugate ionospheres. Such a transient response scenario has been modeled by Kan *et al.* (1982) Kan and Sun (1985), and Rothwell *et al.* (1986, 1988). Kan *et al.* (1982) and Kan and Sun (1985) considered the response of a flux tube to an impulse by considering the time delay between the equatorial plane and the ionosphere and employing the reflection condition given by Equation (41) at the ionosphere and a profile of reflection coefficients in the equatorial plane which is $+1$ on closed field lines and -1 on open field lines. This model produced Pi2-type waveforms, although due to the discrete nature of the input pulse, the waveforms were steplike. This model also used the steady-state version of the conductivity continuity equation (27), and so the waves were generated in the outer magnetosphere rather than being excited by the feedback instability. The excitation of Pi2's by the feedback instability was investigated in the context of the westward traveling surge by Rothwell *et al.* (1986, 1988). They solved the dispersion relation (49) for a spectrum of modes, and superposed these modes to determine a simulated Pi2 observations, which had more realistic smooth profiles than in the steplike model of Kan and Sun (1985).

The generation of pulsations by the feedback instability has been considered in a more realistic geometry by Lysak (1986), who performed a two-dimensional simulation, modeling a flux tube in latitude and altitude, assuming homogeneity in the longitudinal direction. In this work, the dependence of the Alfvén speed on altitude was included, and it was found that the feedback instability could give rise to fast pulsations caused by reflections from relatively low altitudes rather than from the equatorial plane. These

pulsations, in the 1 s period range, were associated with the so-called PiB pulsations (Untiedt *et al.*, 1978: Kangas *et al.*, 1979; Opgenoorth *et al.*, 1980; Bösinger *et al.*, 1981). These waves represent excitations of a resonant cavity formed by the rapid rise of the Alfvén speed from the inosphere to the 2 R_E region (Lysak, 1988). These models indicate that both Pi2 and PiB pulsations are produced by the feedback instability whenever the current system changes dramatically, such as at the head of the westward traveling surge.

6. Field-Aligned Current Generation

The models presented above have all implicitly assumed a generator for the field-aligned current system which exists in the outer magnetosphere. Such a generator must tap the kinetic energy of the magnetospheric plasma and convert it to the electromagnetic energy of the auroral current system. Thus we are led to a situation where electromagnetic energy is generated in the outer magnetosphere and transmitted as a Poynting flux to the acceleration region and the ionosphere, where it is dissipated. The V-shaped equipotential contours often drawn to illustrate auroral fields constitute a transmission line which can transport this energy (Mozer *et al.*, 1980). It has been argued (e.g., Cornwall and Chiu, 1982; Coroniti, 1985) that resistive parallel potential drops are too dissipative to be present on auroral field lines. These arguments neglect the presence of a large-scale Poynting flux transporting energy from the boundary layer to the acceleration region.

On the phenomenological level, one often speaks of current or voltage generators. The consequences of such generators will be discussed in the first subsection. More physically, the description of the auroral current generator may be discussed in terms of the MHD equations (e.g., Vasylianus, 1970), or in terms of multiple fluid equations (Harel *et al.*, 1981; Wolf and Spiro, 1985). An MHD model including the effects of coupling to the ionosphere has recently been presented (Lotko *et al.*, 1987) which can unify a number of the concepts presented in this review. In addition, the boundary-layer plasma is commonly in a turbulent state, leading to the possibility of turbulent dynamo processes which can lead to current generation. These models will be discussed in the second subsection.

6.1. Current and voltage generators

It is useful in considering time-dependent models of the auroral current system to distinguish between generators which deliver a fixed current, and those in which the voltage is fixed. In general, field-aligned currents flow in the auroral zone because currents perpendicular to the background magnetic field in the outer magnetosphere have a non-zero divergence, requiring the closure current to flow along field lines. One can consider two extreme cases. In one case, the perpendicular current, caused for example by diamagnetic or gradient/curvature drifts, is fixed, and the magnetospheric convection pattern changes in order to accommodate this amount of current. On the other hand, we could consider the convection pattern to be fixed. Since the convection is given by the $\mathbf{E} \times \mathbf{B}$ drift, this is equivalent to assuming a potential pattern in the outer

magnetosphere. In this case, the perpendicular current adjusts to maintain the convection. These two extremes may be visualized by a circuit analogy, in which the generator is a battery with an internal resistance. If the internal resistance is small compared to the load on the circuit, the load will receive a fixed voltage; whereas if the load is small compared to the internal resistance, a fixed current, determined by the internal resistance, will be delivered to the load.

The distinction between voltage and current generators becomes important when one considers the reflection of Alfvén waves which propagate from the ionosphere back to the generator. In the case of the voltage generator, the reflection must be in such a sense that the electric field remains constant at the generator, i.e., the reflected wave must have an electric field opposite in sign to the incident wave. Similarly, a wave reflected from a current generator must have a current with the opposite sign as the incident wave. By Equation (40), the current for a downgoing wave has the opposite sign as a current for an upgoing wave with the same electric field. This implies that a wave reflected from a voltage (current) generator has the same sign of current (electric field) as the incident wave.

Figure 10 shows the evolution of current and electric field for both current and voltage generators when a wave is launched from the generator and is incident on a conducting ionosphere (Lysak and Dum, 1983). In the voltage case, the imposed electric field propagates toward the ionosphere, where it is reflected in accordance with Equation (41). The reduced electric field propagates back toward the generator, where

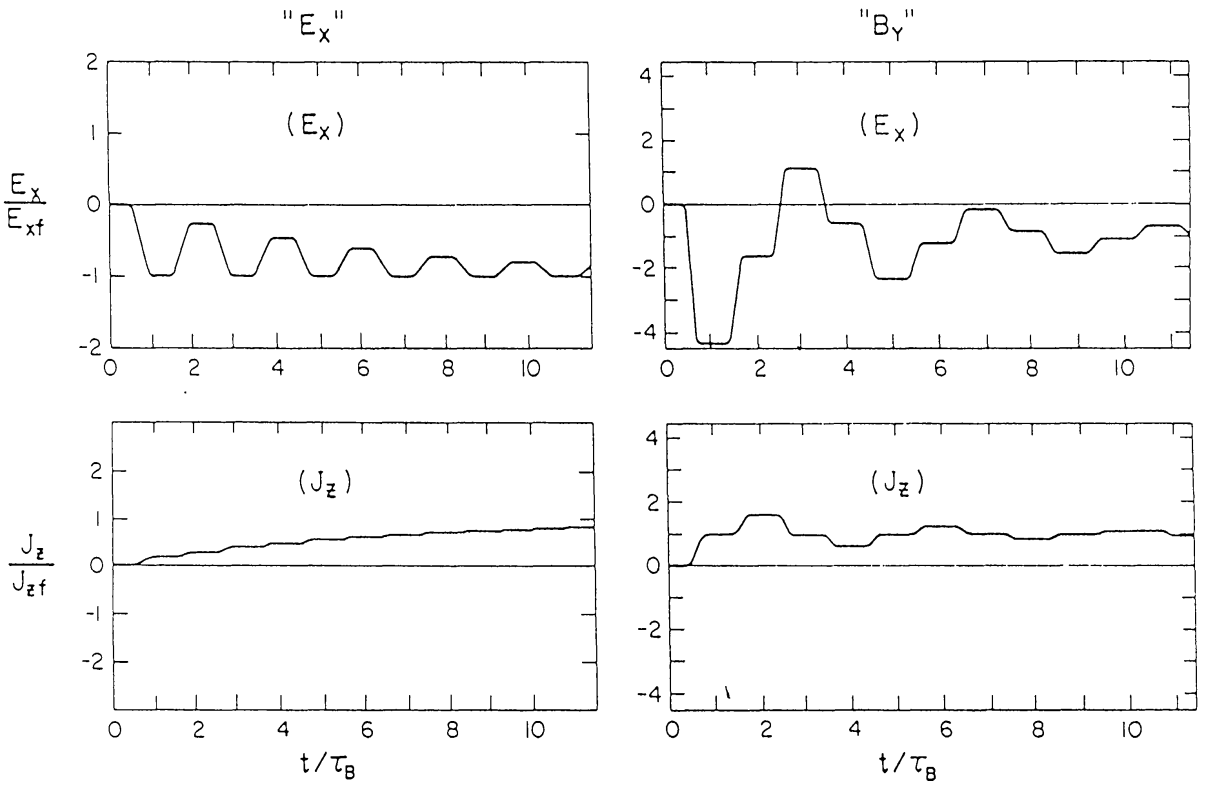

Fig. 10. Time history of perpendicular electric field and field-aligned current for voltage-driven ('E_x') and current-driven ('B_y') runs (from Lysak and Dum, 1983).

it is again reflected so as to maintain the electric field. After a number of reflections, the imposed electric field value is maintained along the entire flux tube. The field-aligned current is increased on each bounce until it reaches the value given by the ionospheric conductivity. The current-driven run evolves much differently. Since the Alfvén conductivity is lower than the ionospheric Pedersen conductivity, the initial electric field is much higher than the steady-state value. Upon reflection from the ionosphere, the electric field is reduced as before, and the current is increased above the imposed value. The reflection from the generator reduces the current back to the imposed value, and the electric field is reversed in sign. Again after a number of bounces, the transient fields are damped out by the ionospheric conductivity and a steady-state is achieved. Note that in the current-driven case, the electric field and current oscillate with a period of $4\tau_B$, where τ_B is the travel time of the Alfvén wave from the generator to the ionosphere, while for the voltage generator, the electric field oscillates at $2\tau_B$. If one considers the generator to be on the equatorial plane of a closed field line, the current generator corresponds to the fundamental oscillation of the field line, while the voltage generator corresponds to the first harmonic.

A useful trick in comparing the properties of current and voltage generators is to introduce an effective conductivity for the generator, which plays the same role as the internal resistance of a battery in the circuit analogy given above. Such a conductivity was introduced by Sonnerup (1980) in order to represent the influence of ionospheric coupling on boundary-layer flow. This conductivity may also be considered to result from Alfvén wave propagation in the generator region, including the result of the deceleration of the convection in the generator (Lysak, 1985). Use of this conductivity is of particular value in numerical models, where by setting the generator conductivity equal to the Alfvén conductivity, an absorbing boundary condition can be implemented. This follows since Alfvén waves incident on the generator will reflect according to the reflection formula (41), with the Pedersen conductivity replaced by the generator conductivity. Again invoking the circuit analogy, it can be seen that high generator conductivity (low internal resistance) corresponds to a voltage generator while low conductivity (high internal resistance) corresponds to a current generator.

The generator conductivity can lead to a modification of the coupling scale length given in Section 4. Consider the generator to be a slab as in Figure 11, with a current $j_{\parallel 0}$ incident on the slab, which has a conductivity Σ_G. Then the integration of the current continuity equation over this slab will yield:

$$j_{\parallel} = j_{\parallel 0} + \Sigma_G \nabla^2 \Phi_0 \,. \tag{53}$$

If Equation (53) is combined with the ionospheric continuity equation (20) and the field-aligned current-voltage relation (21), we can write

$$\left[1 - \frac{\Sigma_G \Sigma_P}{K(\Sigma_P + \Sigma_G)} \nabla^2\right] j_{\parallel} = \frac{\Sigma_P j_{\parallel 0}}{\Sigma_P + \Sigma_G} \,. \tag{54}$$

This equation implies that the magnetosphere-ionosphere coupling scale length L should

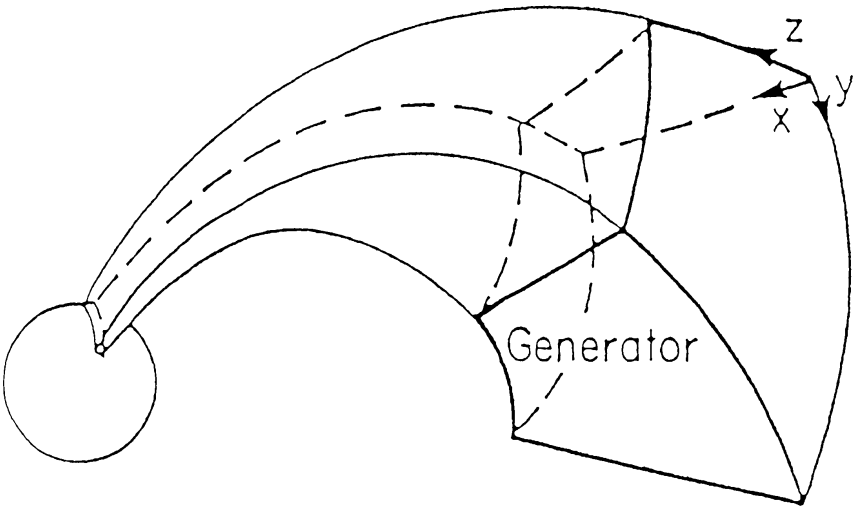

Fig. 11. Sketch of the geometry of auroral field lnes. The generator region is considered to be a slab of height H in the equatorial region (from Lysak, 1985).

be modified to be

$$L = \sqrt{\frac{\Sigma_G \Sigma_P}{K(\Sigma_P + \Sigma_G)}} \,. \tag{55}$$

Note that in the voltage generator case (i.e., $\Sigma_G \gg \Sigma_P$), the scale length reduces to $\sqrt{\Sigma_P/K}$, as determined previously, while for the current generator $L = \sqrt{\Sigma_G/K}$. Thus current generators have a smaller intrinsic scale length associated with them than do voltage generators, indicating that small-scale auroral arcs are more likely to be associated with current than voltage generators. It is also important to note that while Equation (55) has been derived for a straight field line geometry, it can be generalized to arbitrary geometry by mapping the generator conductivity to the ionosphere using appropriate scale factors (Sonnerup, 1980; Lysak, 1985).

There are a number of differences between current systems driven by current and voltage generators. In the current-driven case, the generator electric field (i.e., the convection pattern) is free to adjust to the requirement of current continuity. Lysak (1985) has considered steady-state models of a single current loop imposed on the ionosphere. In the absence of parallel potential drops, this loop would correspond to a single pulse of electric field, or equivalently, to a channel of high-speed convection in the generator region. When this channel has a scale comparable to or smaler than that given by Equation (55), the generator electric field develops reversed field regions, i.e., regions of reversed convection appear on the sides of the initial current channel. Such a structure could correspond to the V-shaped potential contours often invoked for auroral arcs (Gurnett and Frank, 1973; Mozer *et al.*, 1977). On the other hand, for a voltage generator, the convection pattern is fixed and so these V-shaped potentials can not arise spontaneously. Another difference can occur when a current system is imposed on a conductivity gradient. For a pure current generator, the electric field must respond

to this gradient by polarizing so that the electric field is decreased on the high conductivity side, implying $\alpha = 0$ in the terminology of the previous section. On the other hand, for a voltage generator, both the current and the ionospheric electric field can respond, resulting in a large current at the conductivity gradient. It can be shown that the magnetospheric impedance as defined by Equation (46) associated with a generator of conductivity Σ_G is given by (Lysak, 1986):

$$Z = \frac{\Sigma_G + \Sigma_A - (\Sigma_G - \Sigma_A)\, e^{2i\omega T}}{\Sigma_A[\Sigma_G + \Sigma_A + (\Sigma_G - \Sigma_A)\, e^{2i\omega T}]} \,. \tag{56}$$

Observational evidence on the nature of the generator as a function of scale size has been reported by Vickrey *et al.* (1986) who considered seasonal dependences of the current system using data from the HILAT satellite. They found that the strength of the current system on intermediate scales (1–100 km) was independent of season, implying that the ionospheric conductivity did not affect the strength of these currents, as would be the case for a voltage generator. In addition, the electric field was more highly structured in the winter than in the summer, indicating that the electric field was strongly affected by conductivity gradients, which are expected to be more important in the winter hemisphere where precipitation dominates solar illumination as an ionization source for the ionosphere.

It is important to note that the identification of a region as a 'generator' region depends on where the field-aligned current system is closed. If a current system is closed via polarization currents in a wave interference regin such as that shown in Figure 8, it is the Alfvén conductivity in that region which should be used in determining the effective scale size through Equation (55). Since the Alfvén conductivity is very small throughout most of the field line (cf. Figure 7), these low-altitude current closure regions will have the characteristics of current generators. In addition, a resistive parallel electric field regin has a current controlling effect which can cause it to act as a current-like generator. Therefore, models which assume a fixed convection pattern in the equatorial plane are not likely to be able to describe current systems on small and intermediate scales.

6.2. Dynamics of the Boundary Layer

While the generator conductivity model has its usefulness in providing a description of the effects of different types of generators, it does not provide an accurate description of the dynamics of the generator region. A more accurate description can be found by using the MHD equations to describe the plasma flow in this region, and including explicitly the effect of the ionospheric reaction. Early efforts at quantifying this interaction were based on a force balance between the pressure and Lorentz forces (e.g., Vasyliunas, 1970):

$$\nabla p = \frac{\mathbf{j} \times \mathbf{B}}{c} \,. \tag{57}$$

Crossing this equation with $\mathbf{B}$ yields the diamagnetic current $\mathbf{J}_\perp = c\mathbf{B} \times \nabla p / B^2$, and

taking the divergence of this current to yield the parallel current leads to an expression for the field-aligned current at the ionosphere:

$$j_{\parallel} = \frac{B_0}{2B_I}\, c(\nabla p \times \hat{\mathbf{B}}) \cdot \nabla \int \frac{\mathrm{d}l}{B}\,, \tag{58}$$

where B_0 and B_I are the magnetic fields at the source and at the ionosphere, respectively, and the integration is along the field line.

While this model allows steady-state calculations of the convection pattern to be made, it does not include the feedback of the ionosphere on the convection. A model incorporating these effects has been developed by the Rice group (Harel *et al.*, 1981; Wolf and Spiro, 1985). In this model, the field-aligned currents are taken as the divergence of the gradient-curvature currents. The ionospheric continuity equation and Ohm's law are used to determine the electric fields, which are then used to modify the plasma distributions in the outer magnetosphere and again calculate the perpendicular currents. This procedure is repeated cyclically to determine the self-consistent evolution of the current system. This model represents a middle ground between the MHD models and kinetic models, since a multiple fluid approach is used in which ions or electrons in discrete energy ranges are each represented by a fluid. While this model has been successfully compared with data in the inner magnetosphere, it is not applied to the auroral zone and polar cap region since the quasi-static approximation (neglect of the inertial term in the momentum equation) ceases to be valid at higher latitudes.

A complete MHD picture can be used in order to describe the dynamics of these higher latitude regions. The MHD equations (31)–(35) can be simplified in the case of a fluid in the presence of a strong background magnetic field, such as is the case on auroral field lines. In this case, the scale lengths perpendicular to $\mathbf{B}_0$ are much larger than those parallel. In addition, the main fluid motions are the $\mathbf{E} \times \mathbf{B}_0$ motions of the plasma, which are incompressible as long as the parallel magnetic perturbations are negligible (i.e., $\mathbf{B}_0 \cdot (\nabla \times \mathbf{E}) = 0$). Then the pressure can be eliminated from Equation (32) by taking the curl and defining the vorticity $\boldsymbol{\omega} = \nabla \times \mathbf{v}$. Since the velocity is now in the plane perpendicular to the background magnetic field and the parallel gradients are small, the vorticity is primarily in the same direction as $\mathbf{B}_0$, and we can write

$$\rho \frac{\mathrm{d}\omega}{\mathrm{d}t} = \frac{1}{c}\left[\mathbf{b} \cdot \nabla j_{\parallel} + B_0 \frac{\partial j_{\parallel}}{\partial z}\right] + \nu \nabla^2 \omega\,. \tag{59}$$

Similarly, since the magnetic perturbation $\mathbf{b}$ is transverse to the background magnetic field, it can be written in terms of the parallel component of the vector potential $\mathbf{b} = \nabla \times (a\hat{\mathbf{z}})$, which evolves according to

$$\frac{\mathrm{d}a}{\mathrm{d}t} = B_0 \frac{\partial \psi}{\partial z} + \eta \nabla^2 a\,, \tag{60}$$

where ψ is the stream function for the velocity $\mathbf{v} = \nabla \times (\psi \hat{\mathbf{z}})$. These equations were first discussed by and are commonly named for Strauss (1976), and have been discussed by Montgomery (1982) and others. They contain the convective nonlinearity in the plane perpendicular to the background magnetic field, as as the propagation of Alfvén waves along the background field.

While the Strauss equations are naturally suited to discussions of turbulence situations with a strong background magnetic field, there have been only limited investigations of these equations as a model for magnetosphere-ionosphere coupling. The one exception is the work of Seyler (1988) who use a modified form of these equations, incluidng the electron inertial effect which is important for low altitude Alfvén waves (cf. Equation (42)). Seyler finds that the perpendicular magnetic perturbations can give rise to a tearing mode which depends on the inertial length rather than on resistivity. This tearing instability can produce auroral structure even in cases where the Kelvin–Helmholtz instability is stable.

When time-scales longer than the Alfvén transit time are considered, the Strauss equations can be simplified. Lotko *et al.* (1987) have considered such a case as a model for flow in the boundary layer in the presence of ionospheric coupling. They combined Equation (59), integrated over the height of the boundary layer H, with the parallel current-voltage relation (6) and the ionospheric Ohm's Law (20) to form a single equation for the vorticity:

$$(1 - L_i^2 \nabla_i^2)\left(\frac{\partial}{\partial t} + \mathbf{v} \cdot \nabla_{\perp e}\right)\omega = \frac{\Sigma_P B_e}{c\rho B_i}\left(\mathbf{b}_\perp \cdot \nabla_{\perp e} - \frac{B_e}{H}\right)\nabla^2_{\perp i}\Phi_e\,, \tag{61}$$

where the subscripts e and i refer to equatorial and ionospheric quantities, respectively, $\omega = (c\nabla^2_{\perp e}\Phi_e)/B_e$, L_i is the magnetosphere-ionospheric coupling scale length given by (23) and the equatorial and ionospheric quantities are connected by mapping factors. The Fourier transform of Equation (61) can be written in the form:

$$\frac{\mathrm{d}\omega_{\mathbf{k}}}{\mathrm{d}t} = N_{\mathbf{k}} - \Gamma_{\mathbf{k}}\omega_{\mathbf{k}}\,, \tag{62}$$

where $N_{\mathbf{k}}$ is a quadratic nonlinear term and $\Gamma_{\mathbf{k}}$ is a damping rate which can be written as

$$\Gamma_{\mathbf{k}} = \gamma\left[\frac{k^2 L_e^2}{M^2} + \frac{A(\theta)}{1 + k^2 L_e^2 A(\theta)}\right]. \tag{63}$$

Here γ is the damping rate due to ionospheric dissipation:

$$\gamma = \frac{\Sigma_P}{cH\rho}\,\frac{B_e^3}{B_i}\,\frac{\mathrm{d}y_e^2}{\mathrm{d}y_i^2}\,, \tag{64}$$

where $\mathrm{d}y_e/\mathrm{d}y_i$ is the mapping factor in the latitudinal direction. $A(\theta)$ is an anisotropy

factor

$$A(\theta) = \delta \cos^2\theta + \sin^2\theta, \qquad \delta = [(dx_e/dx_i)(dy_i/dy_e)]^2,$$

θ is measured with respect to the x (longitudinal) direction, and M is the Hartmann number given by $M^2 = \gamma L_e^2/\nu$, which measures the radio of Ohmic to viscous dissipation.

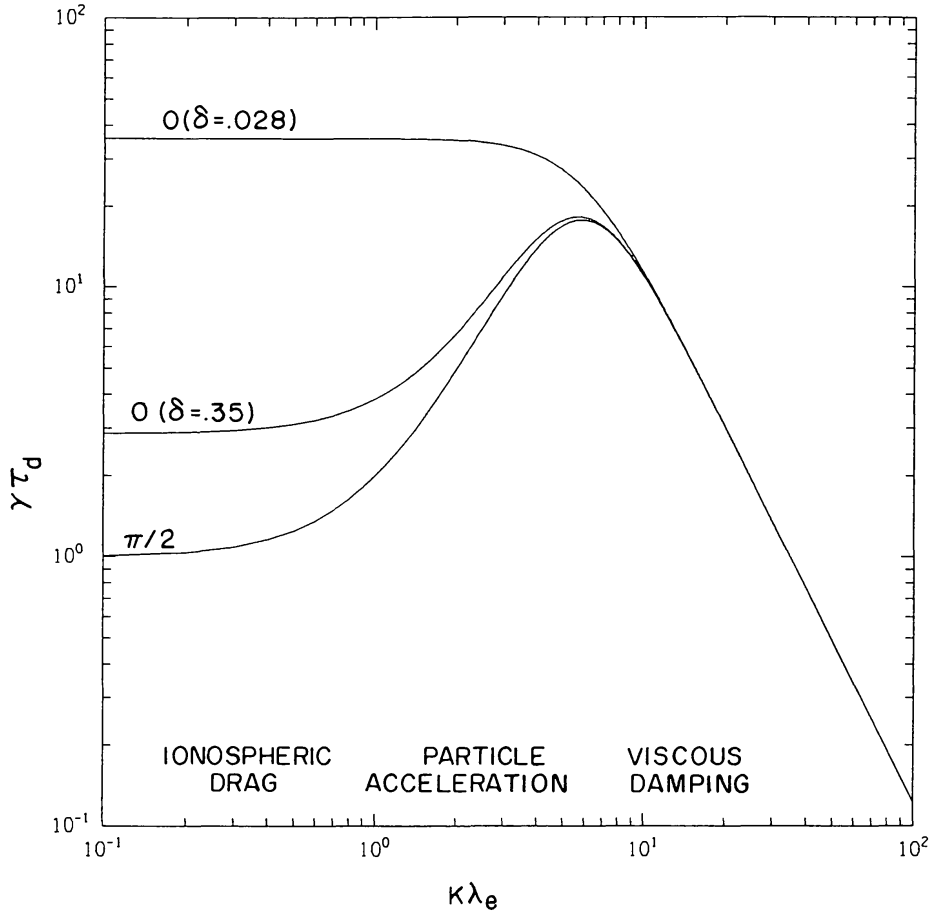

Fig. 12. Normalized damping time $\gamma\tau_d$ for wave vectors lying in the longitudinal ($\theta = 0$) and latitudinal ($\theta = \pi/2$) direction for two different values of the anisotropy factor δ. Note that the latitudinal curve is independent of the anisotropy. Wavelength is normalized to the magnetosphere-ionosphere coupling length at the equator. Ionospheric drag is the dominant dissipation mechanism for long wavelengths, particle acceleration in the parallel electric field dominates at intermediate wavelengths, and viscosity is most important at short wavelengths (from Lotko *et al.*, 1987).

The inverse of the damping rate given by (63), $\tau_d = 1/\Gamma_{\mathbf{k}}$, is plotted in Figure 12. At long wavelengths, the ionospheric damping is dominant and the damping is independent of wavelength and depends on direction as $\Gamma_{\mathbf{k}} = \gamma A(\theta)$. Here this asymmetry is related totally to the anisotropy of the mapping, i.e., a square in the equatorial plane does not map to a square in the ionosphere. At short wavelengths, the damping is due to viscosity and is isotropic, with $\Gamma_{\mathbf{k}} = \nu k^2$. At intermediate wavelengths, there is a minimum in the damping (i.e., a maximum in the lifetime as shown in Figure 12), due to the decoupling of the boundary-layer flow from the ionosphere by parallel electric fields. Note that if there are no parallel electric fields, $L_e = 0$, and the damping rate is a simple superposition

of ionospheric and viscous damping $\Gamma_{\mathbf{k}} = \nu k^2 + \gamma A(\theta)$. When parallel electric fields are present, the minimum damping rate occurs at a wavelength k_* given by $k_* L_e = [M - 1/A]^{1/2}$. In a typical auroral case, $M \gg 1$, and the wavelength of the minimum damping is much less than the original magnetosphere-ionosphere coupling scale. This suggests that small-scale auroral arcs may be associated with large Hartmann number flows. It can also be seen by comparison of Equations (53) and (59) that for viscous-dominated flows, the effective generator conductivity can be written as:

$$\Sigma_G = \frac{H\nu k^2}{V_A} \frac{c^2}{4\pi V_A} . \tag{65}$$

Since the first factor is typically less than unity (see, e.g., the numerical estimates given in Lotko *et al.* (1987)), this model would fall into the class of current generators.

Lotko *et al.* (1987) have discussed a number of one-dimensional solutions of Equation (61) applied to boundary-layer flow and to the dynamics of internal shear layers. Boundary-layer calculation were done by assuming a fixed value of the flow at one boundary and integrating the equations subject to the flow going to zero at infinity. A characteristic overshoot of the convection electric field is found, which scales, for large M, as the minimum damping scale discussed above. Such overshoots are due to the presence of the parallel electric field, much as was discussed above for a current generator. In addition, there is a characteristic displacement of the convection reversal form the equatorial plane to the ionosphere, with the ionospheric convection reversal occurring equatorward of that in the boundary layer. This displacement is essentially due to the filtering of small wavelengths from the ionosphere by the parallel electric field. In the absence of the parallel electric field, or equivalently at low Hartmann number, the thickness of the boundary-layer scales as $(\nu/\Sigma_P)^{1/2}$, similar to the viscous boundary-layer model of Sonnerup (1980). However, in the large Hartmann number regime, the thickness of the boudary layer becomes $(\nu K)^{1/4}$, corresponding to the current-limited model of Sonnerup (1980). Lotko *et al.* (1987) also considered the evolution of a shear layer in which the velocity changes sign and showed that oscillations develop in the convection profile due to the damping out of all waves except those on the minimally damped scale. The resulting electric field structures resemble the V-shock observations of Mozer *et al.* (1977).

The nonlinear terms indicated in Equations (61) and (62) can give rise to a transfer of energy between fluctuations at different scales. These equations, therefore, lead to turbulent phenomena much as those seen in two-dimensional Navier–Stokes turbulence (e.g., Kraichnan and Montgomery, 1980; for reviews of turbulence in the magnetosphere see Kintner and Seyler, 1985; Temerin and Kintner, 1988). In fact, Equation (61) reduces to the Navier–Stokes equations in the limit that the Pedersen conductivity goes to zero, which inhibits any field-aligned current from flowing. It is well known that 2-d Navier–Stokes turbulence undergoes a dual cascade, with enstrophy (mean square vorticity) cascading to smaller scales and energy inverse cascading to large scales. Similar results are found in two-dimensional MHD turbulence, with energy now

participating in the direct cascade and mean-square vector potential having an inverse cascade. The system ocnsidered here represents a state somewhere in between the Navier–Stokes and MHD cases.

When the field-aligned current is weak, the current nonlinearity is not important and the system is close to the Navier–Stokes case. In this limit, Lotko and Schulz (1988) have presented results from a modified Navier–Stokes code which includes the nonlocal damping rate given by Equation (63). They did runs for weak anisotropy ($\delta = 0.35$) and for stronger anisotropy ($\delta = 0.028$). In the weakly anisotropic case, the system formed small eddies with scale sizes comparable with the minimum damping scale. In this case the damping rate has a minimum for both longitudinal and latitudinal perturbations, and roughly isotropic eddies are formed. A k^{-3} enstrophy cascade regime was observed, but the $k^{-5/3}$ inverse cascade was not found, presumably because of strong damping at large scales due to the ionospheric coupling. In the strongly anisotropic case, the longitudinal perturbations are not strongly damped at large scales (cf. Figure 12). In this case, structures extended in the longitudinal direction were formed, and an inverse cascade with approximately the $k^{-5/3}$ power law was seen in the longitudinal wave vectors.

Song and Lysak (1988) have simulated Equation (61) taking into account the full current nonlinearity. They found that the addition of the current nonlinearity accelerated the striation of current filaments with scales equal to and smaller than the minimally damped scales. In addition, there was an indication of an inverse cascade in the magnetic vector potential, indicative of 2-d MHD turbulence. Energy dissipation in the run was reduced from the simple linear case, indicating the existence of a nonlinear transfer of energy to the scales which were minimally damped. This simulation suggests that no matter what the input energy spectrum of turbulence produced by solar wind-magnetosphere coupling processes, in the presence of coupling to the ionosphere the system will tend to evolve to scales comparable with this minimally damped scale.

Although these two-dimensional simulations are useful in illustrating the effect of turbulence on magnetosphere-ionosphere coupling (and *vice versa*), a turbulent picture of current generation can only be done in three dimensions. It is well known (e.g., Moffatt, 1978) that three-dimensional turbulence can give rise to the so-called α-effect, which can generate field-aligned currents. This effect can be illustrated by means of a two-scale model, in which the MHD equations are averaged over the small-scale fluctuations. In this case, the averaged induction equation reads:

$$\frac{\partial \mathbf{B}}{\partial t} = \nabla \times (\mathbf{V} \times \mathbf{B}) + \nabla \times \langle \mathbf{v} \times \mathbf{b} \rangle + \eta \nabla^2 \mathbf{B}\,, \tag{66}$$

where $\mathbf{V}$ and $\mathbf{B}$ represent the large-scale variables and $\mathbf{v}$ and $\mathbf{b}$ the small scales. Since the scale of $\mathbf{B}$ is large, we can take the average term in (66) to be represented as a series in the derivatives of $\mathbf{B}$:

$$\langle \mathbf{v} \times \mathbf{b} \rangle_i = \alpha_{ij} B_j + \beta_{ijk} \frac{\partial B_j}{\partial x_j} + \cdots . \tag{67}$$

In the case of isotropic and homogeneous turbulence, symmetry indicates that we can write $\alpha_{ij} = \alpha\delta_{ij}$ and $\beta_{ijk} = \beta\varepsilon_{ijk}$, leading to the form:

$$\langle \mathbf{v} \times \mathbf{b} \rangle = \alpha\mathbf{B} - \beta\nabla \times \mathbf{B} + \cdots . \tag{68}$$

While the second term gives a contribution to the resistivity, the first leads to an emf parallel to the background magnetic field, which can generate a field-aligned current. Such a current generation can be associated with the formation of loops in the magnetic field configuration formed by velocity shear, e.g., driven by differential rotation in the case of planetary dynamos (Parker, 1970)..

The coefficients α and the turbulent resistivity β, in addition to the eddy viscosity ν, which arises due to the averaging of the $\mathbf{v} \cdot \nabla\mathbf{v}$ and $\mathbf{j} \times \mathbf{b}$ terms in the equation of motion, can be evaluated if the energy and helicity spectra of the kinetic and magnetic fluctuations are known. Early calculation of this type involved the so-called kinematic theory, in which the velocity field was assumed to be fixed. In this case, α and β can be found in terms of the fluctuations of the velocity field (Moffatt, 1978):

$$\alpha = -\frac{1}{3\eta}\int_{k_s}^{\infty} \frac{H_V(k)}{k^2}\,\mathrm{d}k\,, \tag{69}$$

$$\beta = \frac{2}{3\eta}\int_{k_s}^{\infty} \frac{E_V(k)}{k^2}\,\mathrm{d}k\,, \tag{70}$$

where the integral is over the short scales of the fluctuation spectrum, E_V and H_V are the energy and helicity spectra averaged over angle of the velocity field, η is the small-scale resistivity, which is assumed to satisfy $\eta k^2 > \omega$. Note that the α-effect depends on the helicity of the velocity field; a non-helical flow does not give rise to field-aligned current generation.

A number of variants on this basic scheme have been discussed. Fully dynamical theories, in which both the magnetic and kinetic fluctuations are found self-consistently, have been developed both in two dimensions (Biskamp and Welter, 1983; Montgomery and Hatori, 1984) and three dimensions (Montgomery and Chen, 1984; Chen and Montgomery, 1987). In the two-dimensional case, it is found that β depends on the difference between the kinetic and magnetic energy spectra. There is no α-effect for purely 2-d flows. In three dimensions, β is given by (70), but with the microscopic resistivity η replaced by $\eta + \nu$, where ν is the viscosity. The α-effect in three dimensions depends on the difference between the kinetic and magnetic helicities:

$$\alpha = \frac{1}{3(\eta + \nu)}\int_{k_s}^{\infty} \frac{H_B(k) - H_V(k)}{k^2}\,\mathrm{d}k\,. \tag{71}$$

These two-scale theories depend on the existence of a spectral gap clearly separating

the long and short scales. Realistic spectra have no such gap, and are usually smooth across many scales. In this case, the results of two-scale theories can be modified by the renormalization procedure. This procedure consists of performing averages over successively larger scales, and applying the two-scale theory at each step. The limit to a smooth spectrum can then be taken, resulting in a set of coupled differential equations for the transport coefficients (Kichatinov, 1985):

$$\begin{aligned} \frac{d\alpha}{dk} &= \frac{\beta H_V + \alpha E_V}{3\beta^2 k^2} - \frac{H_B}{3\nu k^2} , \\ \frac{d\beta}{dk} &= -\frac{E_V}{3\beta k^2} , \\ \frac{d\nu}{dk} &= -\frac{4E_V}{15\nu k^2} - \frac{3E_B}{15\beta k^2} . \end{aligned} \tag{72}$$

These equations can then be integrated to give the k-dependence of the transport coefficients.

The boundary layer of the magnetopause is known to be a turbulent region in which both the kinetic (electric) and magnetic spectra roughly follow a power law (La Belle and Treumann, 1988; and references therein). The evaluation of the transport coefficients using the equations above is difficult because of the limited nature of the observations, e.g., the helicity spectra. Nevertheless, in a region of strong velocity and magnetic shear such as the magnetopause, it is likely that the turbulence in the boundary layer has finite helicity and is thus capable of establishing a finite α. Simulation results indicating the possible generation of a field-aligned current due to Kelvin–Helmholtz instabilities at the magnetopause have been performed by Miura (1984), although in a two-dimensional simulation such as this, it is not possible to verify the existence of the α-effect from this model. The role of turbulence in the generation of auroral field-aligned currents must, therefore, be considered to be an open question.

7. Summary and Conclusions

In the past ten years, the data from polar orbiting satellites such as S3-3, Dynamics Explorer and Viking have led to an increased understanding of the physical processes which couple the magnetosphere to the ionosphere in the auroral zone. In the picture, the auroral zone can be thought of as a transmission line, carrying electromagnetic energy from a generator region associated with the magnetospheric convection to a load region, including both the Joule dissipation in the ionosphere and the particle acceleration region at higher altitudes. This transmission line is filled with a dielectric which is nonuniform in space due to the variation of the Alfvén speed with altitude, and in which nonlinear losses can take place due to the excitation of plasma turbulence. The transmission line is terminated imperfectly by an ionosphere which generally has a lower

impedance than that of the transmission line. In addition, the ionospheric impedance can also be modified nonlinearly by the energy input which flows down the transmission line. These various feedback processes frequently lead to a non-steady state situation on auroral field lines, which manifests itself in the production of pulsations both in the magnetic field and in particle fluxes.

Observations and models developed in this period have established, at least in the minds of most researchers, that a parallel potential drop is commonly present on the auroral field lines, especially in the duskside region 1 current systems where beams of electrons are accelerated Earthward and beams of ions are accelerated upward. A natural scale length $L = \sqrt{\Sigma_P/K} \approx 100$ km is found, corresponding with the overall scale of the auroral acceleration region. Smaller scale structures within this scale may be associated with different types of generators, as we saw in Section 6. While the zero-order motions of auroral particles can be described using adiabatic theory, wave-particle interactions play a significant role in modifying particle trajectories, producing upward going ion beams and conics, as well as time-varying electron fluxes which cannot be easily generated by adiabatic processes. The modification of the ionosphere itself can give rise to magnetic pulsations since the deposition of energy in the ionosphere can modify the ionospheric impedance and thus change the current pattern. Such feedback interactions are likely to be important in the small-scale dynamics of the aurora, such as the rapid auroral motions which can take place during substorms. Although details of these processes are still under investigation, it is probably safe to say that the fundamental physics of many of these phenomena is basically understood.

Certain aspects of the magnetosphere-ionosphere coupling problem remain to be resolved. The basic underlying mechanisms for the production of the parallel electric field are still controversial, although further analysis of data sets such as that produced by Viking may aid in resolving this issues. Details such as the particular wave modes which are responsible for ion heating and the production of superthermal electron bursts are still open questions, despite extensive research. The generator problem remains quite open, with many of the important issues, such as the development of convection under the influence ionospheric coupling, only beginning to be addressed. The role of turbulence in the generation of currents is also an attractive topic for further research.

This review has discussed the physics of magnetosphere-ionosphere coupling in isolation from the rest of the entire magnetospheric system. Coupling of the solar wind and the magnetosphere at the magnetopause is an important topic intimately related to the question of field-aligned current generation. The so-called flux transfer events (Russell and Elphic, 1979) represent one class of events in which the solar wind-magnetosphere interaction can give rise directly to current generation. Research on the various models of FTEs and their formation and subsequent evolution must eventually be coupled to a discussion of the influence of such structures in the ionosphere. Similarly, the dramatic changes which can occur in the geomagnetic tail, entailing a redistribution of the tail current system, can undoubtedly lead to the production of field-aligned current which couples to the ionosphere. The lack of discussion of such models in this review is not meant to minimize their importance in the overall solar

wind-magnetosphere-ionosphere system, but is due to a lack of space, since discussion of such models could probably fill another review the size of this one.

In summary, the magnetosphere-ionosphere system is a dynamic system which in many ways contains a great deal of interesting physical processes to study. Both MHD and kinetic processes are important in understanding not only the small-scale plasma physical processes, but which also influence the large-scale structure of the current system. The coupling between processes which can be described by plasma kinetic theory and the more global aspects which can more easily be treated by fluid models makes the auroral zone a challenging object of study. Since it is likely that similar current systems and particle acceleration processes are present in other astrophysical processes, such as solar flares, neutron star magnetospheres, accretion disks, and galactic jets, the auroral zone is truly a highly accessible laboratory for studying interesting phenomena throughout the Universe. New observations produced in conjuction with the International Solar Terrestrial Program in the next decade ought to greatly increase our understanding of the magnetosphere-ionosphere system as well as its interactions with the rest of the magnetosphere and the solar wind.

Acknowledgements

The problems outlined in this review first came to my attention at the University of California, Berkeley, during my stay as a graduate student and post-doc during the period when S3-3 satellite was first returning data which has influenced my thinking since. Forrest Mozer, who headed that group, and Mary Hudson, who headed the theoretical effort, created an environment during that period which was highly conducive to the development of a new graduate student in the field. Discussions with my colleagues C. Cattell, C. Carlson, B. Holzworth, B. Lotko, J. Mallinckrodt, M. Temerin, R. Torbert, and J. Wygant during that period were instrumental in developing my interest in this topic and refining my thinking about it. Further development along these lines has benefited greatly by discussions with L. Block, Y. Chiu, P. Christensen, C. Dum, D. Evans, A. Ghielmetti, K. Glassmeier, C. Goertz, D. Gorney, G. Haerendel, J. Hughes, P. Kellogg, P. Kintner, L. Lyons, T. Moore, P. Palmadesso, I. Roth, P. Rothwell, H. Schamel, M. Silevitch, Y. Song, B. Sonnerup, D. Southwood, D. Tetreault, and J. Winckler. There are so many researchers with whom I have discussed the problems outlined in this review that I have undoubtedly forgotten some names, for which I apologize. This work was supported in part by National Science Foundation grants ATM-8451168 and ATM-8508949.

References

Akasofu, S.-I., Kimball, D. S., and Meng, C.-I.: 1965, 'The Dynamics of the Aurora, 2, Westward Travelling Surges', *J. Atmospheric Terr. Phys.* **27**, 173.

Alfvén, H. and Fälthammar, C.-G.: 1963, *Cosmical Electrodynamics*, Clarendon Press, Oxford.

André, M., Koskinen, H., Gustafsson, G., and Lundin, R.: 1987, 'Ion Waves and Upgoing Ion Beams Observed by the Viking Satellite', *Geophys. Res. Letters* **14**, 463.

Arnoldy, R. L.: 1970, 'Rapid Fluctuations of Energetic Auroral Particles', *J. Geophys. Res.* **75**, 228.
Atkinson, G.: 1970, 'Auroral Arcs: Result of the Interaction of a Dynamic Magnetosphere with the Ionosphere', *J. Geophys. Res.* **75**, 4746.
Atkinson, G. and Hutchinson, D.: 1978, 'Effect of the Day-Night Ionospheric Conductivity Grandient on Polar Cap Convective Flow', *J. Geophys Res.* **83**, 725.
Barnes, C., Hudson, M. K., and Lotko, W.: 1985, 'Weak Double Layers in Ion Acoustic Turbulence', *Phys. Fluids* **28**, 1055.
Baumjohann, W. and Glassmeier, K.-H.: 1984, 'The Transient Response Mechanism and Pi2 Pulsations at Substorm Onset – Review and Outlook', *Planetary Space Sci.* **32**, 1361.
Bergmann, R. and Lotko, W.: 1986, 'Transition to Unstable Ion Flow in Parallel Electric Fields', *J. Geophys. Res.* **91**, 7033.
Bergmann, R., Roth, I., and Hudson, M. K.: 1988, 'Linear Stability of the H^+–O^+ Two-Stream Interaction in a Magnetized Plasma', *J. Geophys. Res.* **93**, 4005.
Bernstein, I. B., Greene, J. M., and Kruskal, M. D.: 1957, 'Exact Nonlinear Plasma Oscillations', *Phys. Rev. Letters* **108**, 546.
Bingham, R., Bryant, D. A., and Hall, D. S.: 1984, 'A Wave Model for the Aurora', *Geophys. Res. Letters* **11**, 327.
Birkeland, K.: 1908, *The Norwegian Auroral Polaris Expedition 1902–1903,* Vol. 1, Ascheborg, Christiana.
Biskamp, D. and Welter, H.: 1983, 'Negative Anomalous Resistivity – a Mechanism of the Major Disruption in Tokamaks', *Phys. Letters* **96**, 25.
Block, L. P.: 1972, 'Potential Double Layers in the Ionosphere', *Cosmic Electrodynamics* **3**, 349.
Block, L. P.: 1975, in B. Hultqvist and L. Stenflo (eds.), 'Double Layers', *Physics of the Hot Plasma in the Magnetosphere*, Plenum, New York, p. 229.
Bohm, D.: 1949, in A. Guthrie and R. K. Walkerling (eds.), 'Minimum Ionic Kinetic Energy for a Stable Sheath', *The Characteristics of Electrical Discharges in Magnetic Fields*, McGraw-Hill, New York, p. 77.
Borovsky, J. E. and Joyce, G.: 1983, 'Numerically Simulated Two-Dimensional Auroral Double Layers', *J. Geophys. Res.* **88**, 3116.
Boström, R., Gustafsson, G., Holback, B., Holmgren, G., Koskinen, H., and Kintner, P.: 1988, 'Characteristics of Solitary Waves and Weak Double Layers in the Magnetospheric Plasma', IRF preprint 105.
Bösinger, T., Alanko, K., Kangas, J., Opgenoorth, H., and Baumjohann, W.: 1981, 'Correlations between PiB Type Magnetic Micropulsations, Auroras and Equivalent Current Structures During Two Isolated Substorms', *J. Atmospheric Terr. Phys.* **43**, 933.
Bryant, D. A., Hall, D. S., and Lepine, D. R.: 1978, 'Electron Acceleration in an Array of Auroral Arcs', *Planetary Space Sci.* **26**, 81.
Bujarbarua, S. and Schamel, H.: 1981, 'Theory of Finite Amplitude Electron and Ion Holes', *Plasma Phys.* **25**, 515.
Burch, J. L., Reiff, P. H., Menietti, J. D., Heelis, R. A., Hanson, W. B., Shawhan, S. D., Shelley, E. G., Sugiura, M., Weimer, D. R., and Winningham, J. D.: 1985, 'IMF B_y Dependent Plasma Flow and Birkeland Currents in the Dayside Magnetosphere, 1, Dynamics Explorer Observations', *J. Geophys. Res.* **90**, 1577.
Calvert, W.: 1981, 'The Auroral Plasma Cavity', *Geophys. Res. Letters* **8**, 919.
Chang, T., Hudson, M. K., Jasperse, J. R., Johnson, R. G., Kintner, P. M., Schulz, M., and Crew, G. B. (eds.): 1986, *Ion Acceleration in the Magnetosphere and Ionosphere,* AGU Geophysical Monograph 38, American Geophysical Union, Washington.
Chen, H. and Montgomery, D.: 1988, 'Turbulent MHD Transport Coefficients: an Attempt at Self-Consistency', *Plasma Phys. Controlled Fusion* **29**, 205.
Chiu, Y. T. and Cornwall, J. M.: 1980, 'Electrostatic Model of a Quiet Auroral Arc', *J. Geophys. Res.* **85**, 543.
Chiu, Y. T. and Schulz, M.: 1978, 'Self-Consistent Particles and Parallel Electrostatic Field Distributions in the Magnetospheric-Ionospheric Auroral Region', *J. Geophys. Res.* **83**, 629.
Chiu, Y. T., Newman, A. L., and Cornwall, J. M.: 1981, 'On the Structure and Mapping of Auroral Electrostatic Potentials', *J. Geophys. Res.* **86**, 10029.
Chiu, Y. T., Cornwall, J. M., Fennell, J. F., Gorney, D. J., and Mizera, P. F.: 1983, 'Auroral Plasmas in the Evening Sector: Satellite Observations and Theoretical Interpretations', *Space Sci. Rev.* **35**, 211.
Cornwall, J. M. and Chiu, Y. T.: 1982, 'Effects of Turbulence on a Kinetic Auroral Arc Model', *J. Geophys. Res.* **87**, 1517.

Coroniti, F. V. and Kennel, C. F.: 1972, 'Polarization of the Auroral Electrojet', *J. Geophys. Res.* **77**, 2835.
Coroniti, F. V.: 1985, 'Space Plasma Turbulent Dissipation: Reality or Myth?', *Space Sci. Rev.* **42**, 399.
Croley, D. R., Mizera, P., and Fennell, J. F.: 1978, 'Signature of a Parallel Electric Field in Ion and Electron Distributions in Velocity Space', *J. Geophys. Res.* **83**, 2701.
Dum, C. T. and Dupree, T. H.: 1970, 'Nonlinear Stabilization of High Frequency Instabilities in a Magnetic Field', *Phys. Fluids* **13**, 2064.
Dungey, J. W.: 1963, 'Hydromagnetic Waves and the Ionosphere', *Proc. Int. Conference on the Ionosphere,* Institute of Physics, London, p. 230.
Ellis, P. and Southwood, D. J.: 1983, 'Reflection of Alfvén Waves by Nonuniform Ionospheres', *Planetary Space Sci.* **31**, 107.
Evans, D. S.: 1967, 'A 10 cps Periodicity in the Precipitation of Auroral Zone Electrons', *J. Geophys. Res.* **72**, 4281.
Evans, D. S.: 1974, 'Precipitating Electrons Fluxes Formed by a Magnetic Field-Aligned Potential Difference', *J. Geophys. Res.* **79**, 2853.
Fridman, M. and Lemaire, J.: 1980, 'Relationship Between Auroral Electron Fluxes and Field Aligned Electric Potential Difference', *J. Geophys. Res.* **85**, 664.
Ghielmetti, A. G., Johnson, R. G., Sharp, R. D., and Shelley, E. G.: 1978, 'The Latitudinal, Diurnal, and Altitudinal Distributions of Upward Flowing Energetic Ions of Ionospheric Origin', *Geophys. Res. Letters* **5**, 59.
Ghielmetti, A. G., Sharp, R. D., Shelley, E. G., and Johnson, R. G.: 1979, 'Downward Flowing Ions and Evidence for Injection of Ionospheric Ions into the Plasma Sheet', *J. Geophys. Res.* **84**, 5781.
Ghielmetti, A. G., Shelley, E. G., Collin, H. L., and Sharp, R. D.: 1986, in T. Chang *et al.* (eds.), 'Ion Specific Differences in Energetic Field Aligned Upflowing Ions at 1 R_E', *Ion Acceleration in the Magnetosphere and Ionosphere,* AGU Geophysical Monograph 38, American Geophysical Union, Washington, p. 77.
Glassmeier, K.-H.: 1983, 'Reflection of MHD Waves in the Pc4–5 Period Range at Ionospheres with Nonuniform Conductivity Distributions', *Geophys. Res. Letters* **10**, 678.
Glassmeier, K.-H.: 1984, 'On the Influence of Ionospheres with Nonuniform Conductivity Distribution on Hydromagnetic Waves', *J. Geophys.* **54**, 125.
Goertz, C. K.: 1979, 'Double Layers and Electrostatic Shocks in Space', *Rev. Geophys. Space Phys.* **17**, 418.
Goertz, C. K. and Boswell, R. W.: 1979, 'Magnetosphere-Ionosphere Coupling', *J. Geophys. Res.* **84**, 7239.
Goertz, C. K. and Joyce, G.: 1975, 'Numerical Simulation of the Plasma Double Layer', *Astrophys. Space Sci.* **32**, 165.
Gorney, D. J., Clarke, A., Rowley, D., Fennell, J., Luhmann, J., and Mizera, P.: 1981, 'The Distributions of Ion Beams and Conics Below 8000 km', *J. Geophys. Res.* **86**, 83.
Gurnett, D. A. and Frank, L. A.: 1973, 'Observed Relationships Between Electric Fields and Auroral Particle Precipitation', *J. Geophys. Res.* **78**, 145.
Gurnett, D. A., Huff, R. L., Menietti, J. D., Burch, J. L., Winningham, J. D., and Shawhan, S. D.: 1984, 'Correlated Low-Frequency Electric and Magnetic Noise along Auroral Field Lines', *J. Geophys. Res.* **89**, 8971.
Hanson, W. B.: 1965, in F. S. Johnson (ed.), 'Structure of the Ionosphere', *Satellite Environment Handbook,* Stanford University Press, Stanford, p. 23.
Harel, M., Wolf, R. A., Reiff, P. H., Spiro, R. W., Burke, W. J., Rich, F. J., and Smiddy, M.: 1981, 'Quantitative Simulation of a Magnetospheric Substorm, 1, Model Logic and Overview', *J. Geophys. Res.* **86**, 2217.
Hasegawa, A.: 1976, 'Particle Acceleration by MHD Surface Wave and Formation of Aurora', *J. Geophys. Res.* **81**, 5083.
Hasegawa, A. and Mima, K.: 1978, 'Anomalous Transport Produced by Kinetic Alfvén Wave Turbulence', *J. Geophys. Res.* **83**, 1117.
Heelis, R. A., Hanson, W. B., and Burch, J. L.: 1976, 'Ion Convection Velocity Reversals in the Dayside Cleft', *J. Geophys. Res.* **81**, 3803.
Heelis, R. A., Foster, J. C., de la Beaujardiere, O., and Holt, J.: 1983, 'Multistation Measurements of the High Latitude Ionospheric Convection', *J. Geophys. Res.* **88**, 10111.
Heppner, J. P.: 1972, 'Polar Cap Electric Field Distributions Related to the Interplanetary Field Direction', *J. Geophys. Res.* **77**, 4877.
Hubbard, R. F. and Joyce, G.: 1979, 'Simulation of Auroral Double Layers', *J. Geophys. Res.* **84**, 4297.
Hudson, M. K. and Potter, D. W.: 1981, in S.-I. Akasofu and J. R. Kan (eds.), 'Electrostatic Shocks in the

Auroral Magnetosphere', *Physics of Auroral Arc Formation,* AGU Geophysical Monograph 25, American Geophysical Union, Washington, p. 260.

Hudson, M. K., Lysak, R. L., and Mozer, F. S.: 1978, 'Magnetic Field Aligned Potential Drops Due to Electrostatic Ion Cyclotron Turbulence', *Geophys. Res. Letters* **5**, 143.

Hudson, M. K., Lotko, W., Roth, I., and Witt, E.: 1983, 'Solitary Waves and Double Layers on Auroral Field Lines', *J. Geophys. Res.* **88**, 916.

Hughes, W. J.: 1974, 'The Effect of the Atmosphere and Ionosphere on Long Period Magnetospheric Micropulsations', *Planetary Space Sci.* **22**, 1157.

Iijima, T. and Potemra, T. A.: 1976, 'The Amplitude Distribution of Field-Aligned Currents at Northern High Latitudes Observed by TRIAD', *J. Geophys. Res.* **81**, 2165.

Inhester, B., Baumjohann, W., Greenwald, R. A., and Nielsen, E.: 1981, 'Joint Two-Dimensional Observations of Ground Magnetic and Ionospheric Electric Fields Associated with Auroral Zone Currents, 3, Auroral Zone Currents During the Passage of a Westward Traveling Surge', *J. Geophys.* **49**, 155.

Johnstone, A. D. and Winningham, J. D.: 1982, 'Satellite Observations of Suprathermal Electron Bursts', *J. Geophys. Res.* **87**, 2321.

Kan, J. R. and Lee, L. C.: 1980a, 'On the Auroral Double Layer Criterion', *J. Geophys. Res.* **85**, 788.

Kan, J. R. and Lee, L. C.: 1980b, 'Theory of Imperfect Magnetosphere-Ionosphere Coupling', *Geophys. Res. Letters* **7**, 633.

Kan, J. R. and Sun, W.: 1985, 'Simulation of the Westward Traveling Surge and Pi2 Pulsations During Substorms', *J. Geophys. Res.* **90**, 10911.

Kan, J. R., Longenecker, D. U., and Olson, J. V.: 1982, 'A Transient Response Model of Pi2 Pulsations', *J. Geophys. Res.* **87**, 7483.

Kan, J. R., Williams, R. L., and Akasofu, S. I.: 1984, 'A Mechanism for the Westward Traveling Surge During Substorms', *J. Geophys. Res.* **89**, 2211.

Kangas, J., Pikkarainen, T., Golikov, Yu., Baransky, L., Troitskaya, V. A., and Sterlikova, V.: 1979, 'Bursts of Irregular Magnetic Pulsations During the Substorm', *J. Geophys.* **46**, 237.

Kantrowitz, A. and Petschek, H. E.: 1966, in W. B. Kunkel (ed.), 'MHD Characteristics and Shock Waves', *Plasma Physics in Theory and Application*, McGraw-Hill, New York, p. 148.

Kaufmann, R. L., Ludlow, G. R., Collin, H. L., Peterson, W. K., and Burch, J. L.: 1986, 'Interaction of Upgoing Auroral H^+–O^+ Beams', *J. Geophys. Res.* **91**, 10080.

Kichatinov, L. L.: 1985, 'Renormalization Group Method in Nonlinear Problem of Dynamics of Mean Magnetic Field in a Turbulent Medium', *Magnetohydrodynamics* **21**, 105.

Kindel, J. M. and Kennel, C. F.: 1971, 'Topside Current Instabilities', *J. Geophys. Res.* **76**, 3055.

Kindel, J. M., Barnes, C., and Forslund, D. W.: 1981, in S.-I. Akasofu and J. R. Kan (eds.), 'Anomalous DC Resistivity and Double Layers in the Auroral Ionosphere', *Physics of Auroral Arc Formation,* AGU Geophysical Monograph 25, American Geophysical Union, Washington, p. 296.

Kintner, P. M. and Seyler, C. E.: 1985, 'The Status of Observations and Theory of High Latitude Ionospheric and Magnetospheric Plasma Turbulence', *Space Sci. Rev.* **41**, 91.

Kintner, P. M., Kelley, M. C., and Mozer, F. S.: 1978, 'Electrostatic Hydrogen Cyclotron Waves Near One Earth Radius Altitude in the Polar Magnetosphere', *Geophys. Res. Letters* **5**, 139.

Kintner, P. M., Kelley, M. C., Sharp, R. D., Ghielmetti, A. G., Temerin, M., Cattell, C. A., and Mizera, P. F.: 1979, 'Simultaneous Observations of Energetic (keV) Upstreaming Ions and EHC Waves', *J. Geophys. Res.* **84**, 7201.

Kisabeth, J. L. and Rostoker, G.: 1973, 'Current Flow in Auroral Loops and Surges Inferred from Ground-Based Magnetic Observations', *J. Geophys. Res.* **78**, 5573.

Knight, S.: 1973, 'Parallel Electric Fields', *Planetary Space Sci.* **21**, 741.

Knorr, G. and Goertz, C. K.: 1974, 'Existence and Stability of Strong Potential Double Layers', *Astrophys. Space Sci.* **31**, 209.

Koskinen, H., Boström, R., and Holback, B.: 1988, in T. Chang, G. B. Crew, and J. R. Jasperse (eds.), 'Viking Observations of Solitary Waves and Weak Double Layers on Auroral Field Lines', *Ionosphere-Magnetosphere-Solar Wind Coupling Processes*, Scientific, Cambridge, MA.

Kraichnan, R. H. and Montgomery, D.: 1980, 'Two-Dimensional Turbulence', *Rep. Prog. Phys.* **43**, 547.

LaBelle, J. and Treumann, R. A.: 1988, 'Plasma Waves at the Dayside Magnetopause', *Space Sci. Rev.* **47**, 175.

Lee, L. C. and Kan, J. R.: 1981, in S.-I. Akasofu and J. R. Kan (eds.), *Physics of Auroral Arc Formation*, AGU Geophysical Monograph 25, American Geophysical Union, Washington, p. 245.

Lemaire, J. and Scherer, M.: 1973, 'Plasma Sheet Particle Precipitation: a Kinetic Model', *Planetary Space Sci.* **21**, 281.
Lemaire, J. and Scherer, M.: 1974, 'Ionosphere-Plasma Sheet Field-Aligned Currents and Parallel Electric Fields', *J. Geophys. Res.* **22**, 1485.
Lin, C. S. and Rowland, H. L.: 'Anomalous Resistivity and AE–D Observations of Auroral Electron Acceleration', *J. Geophys. Res.* **90**, 4221.
Lotko, W.: 1983, 'Reflection Dissipation of an Ion-Acoustic Soliton', *Phys. Fluids* **26**, 1771.
Lotko, W.: 1986, 'Diffusive Acceleration of Auroral Primaries', *J. Geophys. Res.* **91**, 191.
Lotko, W. and Kennel, C. F.: 1981, in S.-I. Akasofu and J. R. Kan (eds.), 'Stationary Electrostatic Waves in the Auroral Plasma', *Physics of Auroral Arc Formation*, AGU Geophysical Monograph 25, American Geophysical Union, Washington, p. 437.
Lotko, W. and Kennel, C. F.: 1983, 'Spiky Ion Acoustic Waves in Collisionless Auroral Plasma', *J. Geophys. Res.* **88**, 381.
Lotko, W. and Schulz, C. G.: 1988, in T. E. Moore and J. H. Waite (eds.), 'Internal Shear Layers in Auroral Dynamics', *Modeling Magnetospheric Plasma*, AGU Geophysical Monograph 44, American Geophysical Union, Washington, p. 121.
Lotko, W., Sonnerup, B., and Lysak, R. L.: 1987, 'Nonsteady Boundary Layer Flow Including Ionospheric Drag and Parallel Electric Fields', *J. Geophys. Res.* **92**, 8635.
Lyons, L. R.: 1980, 'Generation of Large-Scale Regions of Auroral Currents, Electric Potentials, and Precipitation by the Divergence of the Convection Electric Field', *J. Geophys. Res.* **85**, 17.
Lyons, L. R. and Waltersheid, R. L.: 1986, 'Feedback Between Neutral Winds and Auroral Arc Electrodynamics', *J. Geophys. Res.* **91**, 13506.
Lyons, L. R., Evans, D. S., and Lundin, R.: 1979, 'An Observed Relation Between Magnetic Field-Aligned Electric Fields and Downward Electron Energy Fluxes in the Vicinity of Auroral Forms', *J. Geophys. Res.* **84**, 457.
Lysak, R. L.: 1985, 'Auroral Electrodynamics with Current and Voltage Generators', *J. Geophys. Res.* **90**, 4178.
Lysak, R. L.: 1986, 'Coupling of the Dynamic Ionosphere to Auroral Flux Tubes', *J. Geophys. Res.* **91**, 7047.
Lysak, R. L.: 1988, 'Theory of Auroral Zone PiB Pulsation Spectra', *J. Geophys. Res.* **93**, 5942.
Lysak, R. L. and Carlson, C. W.: 1981, 'Effect of Microscopic Turbulence on Magnetosphere-Ionosphere Coupling', *Geophys. Res. Letters* **8**, 269.
Lysak, R. L. and Dum, C. T.: 1983, 'Dynamics of Magnetosphere-Ionosphere Coupling Including Turbulent Transport', *J. Geophys. Res.* **88**, 365.
Lysak, R. L. and Hudson, M. K.: 1979, 'Coherent Anomalous Resistivity in the Region of Electrostatic Shocks', *Geophys. Res. Letters* **6**, 661.
Lysak, R. L. and Hudson, M. K.: 1987, 'Effect of Double Layers on Magnetosphere-Ionosphere Coupling', *Laser and Particle Beams* **5**, 351.
Malinckrodt, A. J. and Carlson, C. W.: 1978, 'Relations Between Transverse Electric Fields and Field-Aligned Currents', *J. Geophys. Res.* **83**, 1426.
Maltsev, Yu. P., Leontyev, S. V., and Lyatsky, W. B.: 1974, 'Pi2 Pulsations as a Result of an Alfvén Impulse Originating in the Ionosphere During the Brightening of Aurora', *Planetary Space Sci.* **22**, 1519.
McFadden, J. P., Carlson, C. W., and Boehm, M. H.: 1986, 'Field-Aligned Electron Precipitation at the Edge of an Arc', *J. Geophys. Res.* **91**, 1723.
McFadden, J. P., Carlson, C. W., Boehm, M. H., and Hallinan, T. J.: 1987, 'Field-Aligned Electron Flux Oscillations that Produce Flickering Aurora', *J. Geophys. Res.* **92**, 11133.
McIlwain, C. E.: 1960, 'Direct Measurements of Particles Producing Visible Auroras', *J. Geophys. Res.* **65**, 2727.
Miura, A.: 1984, 'Anomalous Transport by Magnetohydrodynamic Kelvin–Helmholtz Instabilities in the Solar Wind-Magnetosphere Interaction', *J. Geophys. Res.* **89**, 801.
Miura, A. and Sato, T.: 1980, 'Numerical Simulation of the Global Formation of Auroral Arcs', *J. Geophys. Res.* **85**, 73.
Mizera, P. F. and Fennell, J. F.: 1977, 'Signatures of Electric Fields from High and Low Altitude Particle Distributions', *Geophys. Res. Letters* **4**, 311.
Moffatt, H. K.: 1978, *Magnetic Field Generation in Electrically Conducting Fluids*, Cambridge University Press, Cambridge.
Montgomery, D.: 1982, 'Major Disruptions, Inverse Cascades and the Strauss Equations', *Phys. Scripta* **12**, 83.

Montgomery, D. and Chen, H.: 1984, 'Turbulent Amplification and Large-Scale Magnetic Fields', *Plasma Phys. Controlled Fusion* **26**, 1199.

Montgomery, D. and Hatori, T.: 1984, 'Analytical Estimates of Turbulent MHD Transport Coefficients', *Plasma Phys. Controlled Fusion* **26**, 717.

Moses, J. J., Siscoe, G. L., Crooker, N. U., and Gorney, D. J.: 198, 'IMF B_y and Day-Night Conductivity Effects in the Expanding Polar Cap Convection Model', *J. Geophys. Res.* **92**, 1193.

Mozer, F. S.: 1975, in B. M. McCormac (ed.), 'Anomalous Resistivity and Parallel Electric Fields', *Magnetospheric Particles and Fields*, D. Reidel Publ. Co., Dordrecht, Holland, p. 125.

Mozer, F. S. and Fahleson, U. V.: 1970, 'Parallel and Perpendicular Fields in an Aurora', *Planetary Space Sci.* **18**, 1563.

Mozer, F. S., Carlson, C. W., Hudson, M. K., Torbert, R. B., Parady, B., Yatteau, J., and Kelley, M. C.: 1977, 'Observations of Paired Electrostatic Shocks in the Polar Magnetosphere', *Phys. Rev. Letters* **38**, 292.

Mozer, F. S., Cattell, C. A., Hudson, M. K., Lysak, R. L., Temerin, M., and Torbert, R. B.: 1980, 'Satellite Measurements and Theories of Auroral Particle Acceleration', *Space Sci. Rev.* **27**, 155.

Newman, A. L., Chiu, Y. T., and Cornwall, J. M.: 1986, 'Two-Dimensional Quasi-Neutral Description of Particles and Fields Above Discrete Auroral Arcs', *J. Geophys. Res.* **91**, 3167.

Opgenoorth, H. J., Pellinen, R. J., Maurer, H., Kueppers, F., Heikkila, W. J., Kaila, K. U., and Tanskanen, P.: 1980, 'Ground-Based Observations of an Onset of Localized Field-Aligned Currents During Auroral Breakup Around Magnetic Midnight', *J. Geophys.* **48**, 101.

Opgenoorth, H. J., Pellinen, R. J., Baumjohann, W., Nielsen, E., Marklund, G., and Eliasson, L.: 1983, 'Three-Dimensional Current Flow and Particle Precipitation in a Westward Traveling Surge (Observed During the Barium-GEOS Rocket Experiment)', *J. Geophys. Res.* **88**, 3138.

Papadopoulos, K.: 1977, 'A Review of Anomalous Resistivity for the Ionosphere', *Rev. Geophys. Space Phys.* **15**, 113.

Parker, E. N.: 1970, 'The Generation of Magnetic Fields in Astrophysical Bodies, I, The Dynamo Equations', *Astrophys. J.* **162**, 665.

Pashin, A. B., Glassmeier, K.-H., Baumjohann, W., Raspopov, O. M., Yahnin, A. G., Opgenoorth, H. J., and Pellinen, R. J.: 1982, 'Pi2 Magnetic Pulsations, Auroral Break-Up and the Substorm Current Wedge: A Case Study', *J. Geophys.* **51**, 223.

Persson, H.: 1963, 'Electric Field Along a Magnetic Line of Force in a Low-Density Plasma', *Phys. Fluids* **6**, 1756.

Persson, H.: 1966, 'Electric Field Parallel to the Magnetic Field in a Low-Density Plasma', *Phys. Fluids* **9**, 1090.

Peterson, W. K., Shelley, E. G., Boardsen, S. A., and Gurnett, D. A.: 1986, in T. Chang *et al.* (eds.), 'Transverse Auroral Ion Energization Observed on DE-1 with Simultaneous Plasma Wave and Ion Composition Measurements', *Ion Acceleration in the Magnetosphere and Ionosphere,* AGU Geophysical Monograph 38, American Geophysical Union, Washington, p. 43.

Rees, M. H.: 1963, 'Auroral Ionization and Excitation by Incident Energetic Electrons', *Planetary Space Sci.* **11**, 1209.

Reiff, P. H.: 1984, in T. A. Potemra (ed.), 'Models of Auroral Zone Conductances', *Magnetospheric Currents*, AGU Geophysical Monograph 28, American Geophysical Union, Washington, p. 180.

Reiff, P. H., Burch, J. L., and Heelis, R. A.: 1978, 'Dayside Auroral Arcs and Convection', *Geophys. Res. Letters* **5**, 391.

Reiff, P. H., Collin, H. L., Shelley, E. G., Burch, L. J., and Winningham, J. D.: 1986, in T. Chang *et al.* (eds.), *Acceleration in the Magnetosphere and Ionosphere*, AGU Geophysical Monograph 38, American Geophysical Union, Washington, p. 83.

Rishbeth, H. and Garriott, O. K.: 1969, *Introduction to Ionospheric Physics,* Academic Press, New York.

Rostoker, G. and Samson, J. C.: 1981, 'Polarization Characteristics of Pi2 Pulsations and Implications for Their Source Mechanisms: Location of the Source Regions with Respect to the Auroral Electrojets', *Planetary Space Sci.* **29**, 225.

Rostoker, G., Vallance Jones, A., Gattinger, R. L., Anger, C. D., and Murphree, J. S.: 1987, 'The Development of the Substorm Expansive Phase: the "Eye" of the Substorm', *Geophys. Res. Letters* **14**, 399.

Rothwell, P. L., Silevitch, M. B., and Block, L. P.: 1984, 'A Model for Propagation of the Westward Traveling Surge', *J. Geophys. Res.* **89**, 8941.

Rothwell, P. L., Silevitch, M. B., and Block, L. P.: 1986, 'Pi2 Pulsations and the Westward Traveling Surge', *J. Geophys. Res.* **91**, 6921.

Rothwell, P. L., Silevitch, M. B., Block, L. P., and Tanskanen, P.: 1988, 'A Model for the Westward Traveling Surge and the Generation of Pi2 Pulsations', *J. Geophys. Res.* **93**, 8613.

Rowland, H. L. and Palmadesso, P. J.: 1983, 'Anomalous Resistivity Due to Low-Frequency Turbulence', *J. Geophys. Res.* **88**, 7997.

Rowland, H. L., Palmadesso, P. J., and Papadopoulos, K.: 1981, 'Anomalous Resistivity on Auroral Field Lines', *J. Geophys. Res.* **8**, 1257.

Russell, C. T. and Elphic, R. C.: 1979, 'ISEE Observations of Flux Transfer Events at the Magnetopause', *Geophys. Res. Letters* **6**, 33.

Samson, J. C. and Rostoker, G.: 1983, 'Polarization Characteristics of Pi2 Pulsations and Implications for Their Source Mechanism: Influence of the Westward Traveling Surge', *Planetary Space Sci.* **31**, 435.

Sato, T.: 1978, 'A Theory of Quiet Auroral Arcs', *J. Geophys. Res.* **83**, 1042.

Sato, T. and Okuda, H.: 1981, 'Numerical Simulation of Ion Acoustic Double Layers', *J. Geophys. Res.* **86**, 3357.

Schamel, H.: 1972, 'Stationary Solitary, Snoidal, and Sinusoidal Ion Acoustic Waves', *Plasma Phys.* **14**, 905.

Seyler, C. E.: 1988, 'Nonlinear 3-d Evolution of Bounded Kinetic Alfvén Waves Due to Shear Flow and Collisionless Tearing Instability', *Geophys. Res. Letters* **15**, 756.

Shawhan, S. D.: 1984, 'Magnetospheric Plasma Wave Research, 1975–1978', *Rev. Geophys. Space Phys.* **17**, 705.

Song, Y. and Lysak, R. L.: 1988, in T. E. Moore and J. H. Waite (eds.), 'Turbulent Generation of Auroral Currents and Fields – A Spectral Simulation of 2-d MHD Turbulence', *Modeling Magnetospheric Plasma*, AGU Geophysical Monograph 44, American Geophysical Union, Washington, p. 197.

Sonnerup, B. U. O.: 1980, 'Theory of the Low Latitude Boundary Layer', *J. Geophys. Res.* **85**, 2017.

Southwood, D. J. and Hughes, W. J.: 1983, 'Theory of Hydromagnetic Waves in the Magnetosphere', *Space Sci. Rev.* **35**, 301.

Spiro, R. W., Reiff, P. H., and Maher, L. J.: 1982, 'Precipitating Electron Energy Flux and Auroral Zone Conductances: An Empirical Model', *J. Geophys. Res.* **87**, 8215.

Strauss, H. R.: 1976, 'Nonlinear, Three-Dimensional Magnetohydrodynamics of Noncircular Tokamaks', *Phys. Fluids* **19**, 134.

Sugiura, M., Maynard, N. C., Farthing, W. H., Heppner, J. P., Ledley, B. G., and Cahill, L. J.: 1982, 'Initial Results on the Correlation Between the Electric and Magnetic Fields Observed from the DE 2 Satellite in the Field-Aligned Current Regions', *Geophys. Res. Letters* **9**, 985.

Swift, D. W.: 1975, 'On the Formation of Auroral Arcs and the Acceleration of Auroral Electrons', *J. Geophys. Res.* **80**, 2096.

Swift, D. W.: 1978, 'Mechanisms for the Discrete Aurora – A Review', *Space Sci. Rev.* **22**, 35.

Swift, D. W.: 1979, 'An Equipotential Model for Auroral Arcs: the Theory of Two-Dimensional Laminar Electrostatic Shocks', *J. Geophys. Res.* **84**, 6427.

Temerin, M. and Kintner, P. M.: 1988, 'Review of Ionospheric Turbulence', *Proc. Chapman Conference on Plasma Waves and Instabilities*, Sendai, Japan.

Temerin, M., Cattell, C., Lysak, R., Hudson, M., Torbert, R. B., Mozer, F. S., Sharp, R. D., and Kintner, P. M.: 1981, 'The Small-Scale Structure of Electrostatic Shocks', *J. Geophys. Res.* **86**, 11278.

Temerin, M., Cerny, K., Lotko, W., and Mozer, F. S.: 1982, 'Observations of Double Layers and Solitary Waves on Auroral Zone Field Lines', *Phys. Rev. Letters* **48**, 1175.

Tetreault, D. J.: 1988, 'Growing Ion Holes as the Cause of Auroral Double Layers', *Geophys. Res. Letters* **15**, 164.

Untiedt, J., Pellinen, R., Kueppers, F., Opgenoorth, H. J., Pelster, W. D., Baumjohann, W., Ranta, H., Kangas, J., Czechowsky, P., and Heikkila, W. J.: 1978, 'Observations of the Initial Development of an Auroral and Magnetic Substorm at Magnetic Midnight', *J. Geophys.* **45**, 41.

Vasyliunas, V. M.: 1970, in B. McCormac (ed.), 'Mathematical Models of Magnetospheric Convection and Its Coupling to the Ionosphere', *Particles and Fields in the Magnetosphere*, D. Reidel Publ. Co., Dordrecht, Holland, p. 29.

Vickrey, J. F., Livingston, R. C., Walker, N. B., Potemra, T. A., Heelis, R. A., Kelley, M. C., and Rich, F. J.: 1986, 'On the Current-Voltage Relationship of the Magnetospheric Generator at Intermediate Spatial Scales', *Geophys. Res. Letters* **13**, 495.

Vickrey, J. F., Vondrak, R. R., and Matthews, S. J.: 1981, 'The Diurnal and Latitudinal Variation of Auroral Zone Ionospheric Conductivity', *J. Geophys. Res.* **86**, 65.

Wallis, D. D. and Budzinski, E. E.: 1981, 'Empirical Models of Height-Integrated Conductivities', *J. Geophys. Res.* **86**, 125.

Watanabe, K. and Sato, T.: 1988, 'Self-Excitation of Auroral Arcs in a Three-Dimensionally Coupled Magnetosphere-Ionosphere System', *Geophys. Res. Letters* **15**, 717.

Weimer, D. R., Goertz, C. K., Gurnett, D. A., Maynard, N. C., and Burch, J. L.: 'Auroral Zone Electric Fields from DE 1 and 2 at Magnetic Conjunctions', *J. Geophys. Res.* **90**, 7479.

Whalen, B. A. and Daly, P. W.: 1979, 'Do Field-Aligned Auroral Particle Distributions Imply Acceleration by Quasi-Static Parallel Electric Fields?', *J. Geophys. Res.* **84**, 4175.

Whipple, E. C.: 1977, 'The Signature of Parallel Electric Fields in a Collisionless Plasma', *J. Geophys. Res.* **82**, 1525.

Wilhelm, K., Bernstein, W., Kellogg, P. J., and Whalen, B. A.: 1985, 'Fast Magnetospheric Echoes of Energetic Electron Beams', *J. Geophys. Res.* **90**, 491.

Witt, E. and Lotko, W.: 1983, 'Ion-Acoustic Solitary Waves in a Magnetized Plasma with Arbitrary Electron Equation State', *Phys. Fluids* **26**, 2176.

Witt, E. and Hudson, M. K.: 1986, 'Electrostatic Shocks as Nonlinear Ion Acoustic Waves', *J. Geophys. Res.* **91**, 11217.

Wolf, R. A. and Spiro, R. W.: 1985, in H. Matsumoto and T. Sato (eds.), 'Particle Behavior in the Magnetosphere', *Computer Simulation of Space Plasmas*, Terra Scientific, Tokyo, p. 227.

Wu, C. S. and Lee, L. C.: 1979, 'A Theory of Terrestrial Kilometric Radiation', *Astrophys. J.* **230**, 621.

Yasuhara, F., Greenwald, R., and Akasofu, S.-I.: 1983, 'On the Rotation of the Polar Cap Potential Pattern and Associated Polar Phenomena', *J. Geophys. Res.* **88**, 5773.